AMERICAN UNIVERSITY OF BEIRUT

ENHANCED BLACK HOLE PARTICLE SWARM OPTIMIZATION IN WELL PLACEMENT OPTIMIZATION

by
YARA YOUSSEF BOU NASSIF

A thesis
submitted in partial fulfillment of the requirements
for the degree of Master of Science
to the Department of Chemical Engineering and Advanced Energy
of the Maroun Semaan Faculty of Engineering and Architecture
at the American University of Beirut

Beirut, Lebanon
January 2021

AMERICAN UNIVERSITY OF BEIRUT

ENHANCED BLACK HOLE PARTICLE SWARM OPTIMIZATION IN WELL PLACEMENT OPTIMIZATION

by

YARA YOUSSEF BOU NASSIF

Approved by:

Kassem Ghorayeb 

Dr. Kassem Ghorayeb, Assistant Professor — Advisor
Chemical Engineering and Advanced Energy

Kassem Ghorayeb, on behalf of Dr. Joseph Zaiter 

Dr. Joseph Zeaiter — Member of Committee

Kassem Ghorayeb, on behalf of Dr. Elsa Maalouf 

Dr. Elsa Maalouf — Member of Committee

Kassem Ghorayeb, on behalf of Dr. Georges Saad 

Dr. George Saad — Member of Committee

Date of thesis defense: [January 27, 2021]

AMERICAN UNIVERSITY OF BEIRUT

THESIS RELEASE FORM

Student Name:	Bou Nassif	Yara	Youssef
	Last	First	Middle

I authorize the American University of Beirut, to: (a) reproduce hard or electronic copies of my thesis; (b) include such copies in the archives and digital repositories of the University; and (c) make freely available such copies to third parties for research or educational purposes:

- [x] As of the date of submission
- [ ] One year from the date of submission of my thesis.
- [ ] Two years from the date of submission of my thesis.
- [ ] Three years from the date of submission of my thesis.

Yara Bou Nassij	January 29,2021
Signature	Date

ACKNOWLEDGEMENTS

Jesus, thank you for always watching over me, for guiding me every step of the way and for always placing just the right people in my path. Dr. Kassem, it has been a pleasure and a blessing to have worked with you. Your love and dedication for what you do radiates and motivates all who meet and work with you. Ahmad, thank you for your guidance and patience throughout it all. Racha, I will always hold our late-night tea sessions in Oxy dear to my heart. Haytham, you applauded me for the smallest milestones that I would cross and for that I will always be grateful. Hussein, you're a genius. Saloma, you made being away from home feel like home. Aseel, Hassan, and Elie, you've been here from the beginning, I pray that no matter where life takes me, I'll always have you guys by my side. Roy and Luke, my two younger brothers, I have so much to be thankful to you guys for, so I'm going to leave it at, as they say in Arabic, bhebkon.

Mum and dad, this one is for you. I know I have not always been the easiest child to deal with but thank you for your constant support and love. Thank you for always catching me first and being the shoulder that I lean on during my one too many breakdowns in the past 7 years of my university life. Thank you for always pushing me to do my best and teaching me to take a step back and breathe when things get a little rough. I love you forever.

ABSTRACT
OF THE THESIS OF

Yara Youssef Bou Nassif for Master of Science
Major: Chemical Engineering

Title: Enhanced Black Hole Particle Swarm Optimization in Well Placement Optimization

Engineers and geoscientists work within an asset team on defining well type, well control, well placement and facility design towards optimizing the development planning of oil and gas fields. Well placement optimization plays a critical role in field development planning, since it accounts for a major portion of the capital expenditure and significantly affects hydrocarbon recovery. This thesis presents an updated version of the black hole particle swarm optimization (BHPSO), a well placement evolutionary optimizer introduced by Harb et al. [1]. BHPSO simultaneously optimizes the well count, location, type, and trajectory of wells. The importance of the proposed algorithm is that while well placement optimization involves a large number of optimization parameters, the BHPSO drastically reduces the number of optimization variables as its computational complexity is independent of the number of optimized wells. Harb et al. [1] focused on pattern water injection. In this research project, we address a different injection scheme: peripheral water injection. Here, for each particle in a BHPSO "iteration", the particle swarm optimization (PSO) defines the location of the first producer based on a net hydrocarbon thickness (NHCT) map, and the location of the first injector is determined based on the permeability thickness (Kh) map of the field. The number of the remaining wells is decided by the PSO and, then, using the black hole (BH) operator, producers are automatically and optimally placed using a NHCT map, followed by the placement of the injectors on a Kh map. After every well placement, the maps are updated by eliminating a black hole (a disk and/or a cylinder) around the producers and injectors, each on the relevant map respectively. The radius of the black hole is defined by the well spacing. The method was extensively tested on both the synthetic Olympus reservoir model and the PUNQ-S3 reservoir model. Additionally, a new black holing technique was introduced and tested in the process of further optimizing the BH operator results. Furthermore, the convergence criteria of PSO is addressed in this study by conducting a sensitivity analysis on its algorithmic parameters including the acceleration factors, and the swarm size. The Inertia weight, another algorithmic parameter of PSO, was changed from a Constant Inertia Weight to a Linearly Decreasing Inertia Weight (LDIW). The latter showed improved results over the former in terms of convergence as faster convergence was obtained using a LDIW.

TABLE OF CONTENTS

ILLUSTRATIONS

Figure

TABLES

Table

CHAPTER 1

LITERATURE REVIEW

In field development planning, engineers and geoscientists work on defining well type, well control, well placements, and facility design [2]. Data extracted from seismic surveys, cores, logs, fluid samples, well testing and production/injection/pressure history is studied and analyzed for building static and dynamic models that are used to test different development strategies, forecast production, and decide on the optimal field development plan [2]. These development strategies are ranked based on economic indicators, oil recovery, risk, and availability of injection fluids [3]. Also, the field development plan could be modified or adjusted throughout the productive life of the field for several reasons such as poor production performance, economics, new technologies (well types or recovery processes), environmental constraints, and better understanding of the reservoir due to the reduction of uncertainties with time [3].

One of the most important decisions that significantly impact the recovery performance and profitability of a reservoir is the placement of production and injection wells. Therefore, the optimization of well placement is crucial in achieving an optimal field development plan [4]. Well placement optimization is a process used to determine several variables including optimal well location, well count, type, and injection pattern, towards maximizing a predefined objective function i.e. NPV, Oil cumulative production, plateau length etc... [1]. However, the computational requirement for achieving well placement optimization is very high due to the large number of simulations needed to test the different combinations of the decision variables involved.

Computational requirements may become prohibitively expensive within the context of a real oil or gas field development planning project. Hence, finding an efficient algorithm that can reduce the computation load of this process is a great benefit to the industry [5]. Consequently, in the past decade, substantial research focused on automating and developing optimization algorithms for well placement optimization.

1.1. Well Placement Optimization

The emergence of optimization algorithms in field development optimization can be dated back to the early 1990s [6]. In a review conducted by Islam et al. [5] the numerous artificial intelligence techniques for well placement optimization problems were compared and discussed. Due to reservoir heterogeneities, well placement problems yield cost functions that are discontinuous, non-smooth, nonconvex, and contain multiple local optima [5]. Well placement optimization challenges can be attributed to the aforementioned points; hence it is critical to find a practical algorithm to tackle this complexity. The optimization algorithms presented in Figure 1 were utilized in well placement optimization problems. These algorithms can be classified into 3 main groups: Classical Techniques (Gradient Based), Non-Classical Techniques (Gradient-free), and Hybrid Techniques.

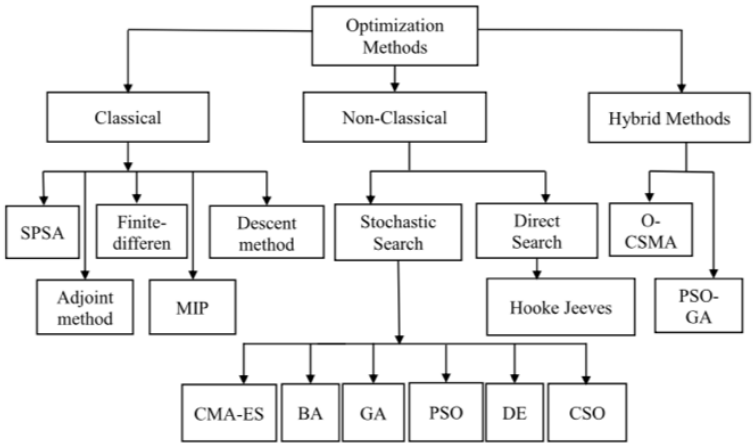

Figure 1 Algorithms used for Well Placement Optimization [5]

The drawbacks of gradient based algorithms are: (1) they often get trapped in a local optimum, and (2) the gradient of some models is difficult to estimate. On the other hand, gradient-free algorithms have a better tendency to be freed of the local optima. They also do not require derivative calculation and hence can work with the model as a "black box" [5]. Over time, as gradient based algorithms did not prove to be sufficient on their own in optimizing well locations, researchers decided to combine the 2 main groups of algorithms: gradient-based and gradient-free algorithms resulting in the third group: Hybrid Techniques. The Hybridization of algorithms has proved to work better than stand-alone algorithms in some cases [5].

Many breakthroughs were made over the past decade in well placement optimization. In 2010, Onwualu & Durlofsy [7] introduced Particle Swarm Optimization (PSO) to this field. In their work, the performance of optimizing well location and type using PSO and GA were compared in which they concluded that PSO outperforms GA. Nevertheless, it was stated that the methods were particularly case dependent and went on to propose, a year later, an optimization procedure for large scale field development called Well Pattern Optimization (WPO). The WPO comprises

2 key components: Well Pattern Description (WPD) & Well to Well Perturbation (WWP). The core algorithm used within the WPO is PSO. WPD encodes solutions with regard to well patterns (5-spot, 9-spot, etc) and pattern operators rather than individual well placement, and so the parameters optimized were affiliated with pattern type and geometry [8]. Since the optimization variables were dependent on different well patterns rather than the wells considered, the amount of optimization parameters was significantly reduced. While the optimization of the pattern type and geometry were optimized under the WPD representation, the optimization of the location of wells within each pattern can be optimized under the WWP representation. When the NPV obtained using the WPO was compared to the NPV of that of a standard well pattern scenario, the WPO yielded significantly larger NPVs [8]. In 2016, Zhang et al. [9] published a work based on the idea presented by Onwualu & Durlofsy. In order to reduce optimization complications, Zhang et al [9] narrowed down the number of optimization parameters of the WPO by eliminating parameters that they deemed unnecessary. Accordingly, they were able to test a perturbation gradient algorithm to accelerate the speed of simulation time. In order to validate the gradient algorithm, experiments were carried out on both a homogenous and a heterogeneous reservoir leading to satisfactory results for the homogenous reservoir. As for the heterogenous reservoir, the gradient algorithm resulted in faster convergence than the PSO, however, as the well placement optimization problem is convex, the gradient algorithm returned some “unreasonable” results. In other words, they concluded that convex optimization problems with complicated objective function surfaces highly limit gradient optimization methods [9]. The PSO’s instability (non-uniqueness of solution) was also

highlighted by Zhang et al [9], stating that PSO is starting point dependent and yields different results at different times using the same particle number.

While PSO was introduced to well placement optimization in 2010, a relatively new algorithm known as Artificial Bee Colony (ABC), was shed light on in 2016 in a study carried out by Nozohour-leilabady and Fazelabdolabadi [10]. ABC is a swarm based stochastic optimization method that is used for global optimization and can handle both constrained and unconstrained optimization problems [6]. Nozohour-leilabady and Fazelabdolabadi [10] used the ABC optimization algorithm to optimize over well locations and types. In order to validate the ABC method and compare its performance with PSO, the authors used different reservoir models with randomly generated permeability. The results obtained proved that the ABC optimization algorithm outperformed PSO with regard to finding the global optimum. The ABC's excellence was attributed to it being starting point independent, an attribute PSO lacks [10]. While the ABC algorithm is deemed promising for application in well placement optimization, it is limited by its 'out-of-boundary' solution vectors. This limitation causes the algorithm to produce, at some point, 'new' solutions outside of the search space (i.e. solutions outside the defined boundaries of the problem) [10,11]. The aforementioned issue results in solution vectors that are not considered for NPV calculations, and while the default treatment for this problem is either to place the points back in the search space (at the boundary) or to disregard them, it is inefficient [10]. However, in 2018, Udoeyop, Oboh, and Afiakinye [11] carried out a study which lead to a modified ABC (MABC) algorithm in which they addressed the 'out-of-boundary' solutions, a task Nozohour-leilabady and Fazelabdolabadi [10] did not undertake. The MABC proved to converge faster than the ABC algorithm, towards a

global maximum solution, as it was not repeating iterations that had already been generated but were located outside the search space. Furthermore, Udoeyop, Oboh, and Afiakinye [11] went on to verify the algorithms' (MABC & ABC) independence of the starting point and concluded that the MABC algorithm is a more efficient optimizer, and that it surpassed the ABC algorithm in terms of the results obtained. Even though MABC was shown to outperform ABC, which in turn was shown to outperform PSO, it must be noted that both algorithms did not account for the optimization of well count.

In 2019, Harb et al. [1] developed a new hybrid evolutionary optimization method for well placement. Where Onwualu & Durlofsy [8] combined the well pattern operator with the PSO algorithm, Harb et al. [1] combined it with a Black Hole Operator resulting in the Black Hole Particle Swarm Optimization (BHPSO).The main focus of the BHPSO is on optimizing the well count, location, type, and trajectory of the well. A quality map known as the NHCT map was used to place the wells, and it is an indication of the thickness of oil at a certain point in the reservoir. The PSO identifies the location of the first well based on the NHCT map. Once the location of the first well has been identified, the BHO automatically and optimally places the remaining wells on the map based on the highest NHCT value [1]. After every well placement, the map is updated by eliminating a disk which is referred to as the black hole. The radius of the disk is defined by the well spacing. Since the first well is the only well that is being placed by the PSO, then the PSO algorithm initializes the solution vector for the BHO. Harb et al. [1] developed an equation called the Technical Well Spacing (TWS) which was exclusively used for the BHPSO to ensure that all the wells would have a place on the NHCT map which in turn made the algorithm independent of the number of optimized wells [1]. Harb et al. [1] conducted a sensitivity to compare between BHPSO

and PSO in terms of problem complexity, swarm size, and stochastic nature of the core algorithm. The NPV was used as the objective function for both algorithms. It was found that BHPSO outperformed PSO with a 40-50% increase in the BHPSO NPV's when compared to the PSO NPV's [1]. BHPSO also surpassed PSO in terms of CPU. The work that was presented focused on optimizing pattern water injection schemes, with a future focus on peripheral water injection schemes and convergence criteria.

1.2. Peripheral Water Injection Schemes

1.2.1. Recovery Mechanisms

Water injection schemes are a form of secondary recovery mechanisms. Recovery mechanisms are used to maximize the recovery of hydrocarbons from a reservoir and fall under 2 headings: Conventional Recovery which includes primary and secondary recovery mechanisms, and Enhanced Oil Recovery (EOR) which is typically a tertiary recovery mechanism. Hydrocarbons are first displaced from the reservoir by natural depletion as a result of the energy that is initially present in the reservoir [12]. Natural depletion of oil recovers up to 25% of the oil initially in place depending on may factors [12]. As the initial pressure in the reservoir decreases to pressures near those needed to flow oil/water to the wellbore, artificial lift methods can be used to reduce the bottom hole pressure and help "lifting" the oil to the surface. These artificial lift techniques are wellbore centric and do not address the bigger picture of enhancing recovery from the reservoir. The technical limit of the primary recovery mechanism stage is reached when the pressure in the reservoir significantly drops to the point where production rates are no longer economical.

Secondary recovery mechanisms come in the form of adding artificial energy to the reservoir by means of a well while producing oil/gas/water by means of another well [12]. Energy is added to the reservoir by injecting either water or gas and is referred to as pressure maintenance. Pressure maintenance slows down the pressure decline in a reservoir and results in increased oil recovery [13]. The limit of the secondary recovery mechanism stage is reached when the fluid injected into the reservoir is produced in substantial amounts (e.g. high water cut or gas-to-oil-ratio) leading to uneconomical production.

Tertiary recovery is an attempt to recover oil past primary and secondary recovery. The parameters that govern the recovery of the oil are altered by using thermal, microbial, (miscible) gas or chemical injection techniques to increase the recovery factor by, typically, reducing the irreducible oil saturation [14]. Recovery of oil can further be improved by 5-10% by implementing such tertiary recovery mechanisms [14].

1.2.2. Injection Schemes

Injection schemes play a significant role in maximizing oil production revenues. For this role to be achieved, injection scheme projects should lead to both maintaining the reservoir pressure and maximizing the sweep efficiency in the reservoir which in turn leads to increasing the oil recovery. Sweep efficiency depends on the volume and heterogeneity of the reservoir that is contacted by the injected fluid as well as the type of injection scheme selected for the reservoir [15]. The four general types of injection schemes are:

1. Irregular Pattern Injection: Simplest type of injection in which the wells can be placed in any manner or pattern that is suitable for injection.
2. Pattern Injection: the injector wells are placed in repeated patterns throughout the field as shown in Figure 2.

   Common pattern injection schemes are:

   - Direct Line Drive
   - Staggered Line Drive
   - Normal 5-Spot/Inverted 5-Spot
   - Normal 7 Spot/Inverted 9-Spot
   - Normal 9-Spot/Inverted 9-Spot

   Normal patterns are patterns that have only one production well per pattern, and inverted patterns are patterns that have only one injection well per pattern [16].

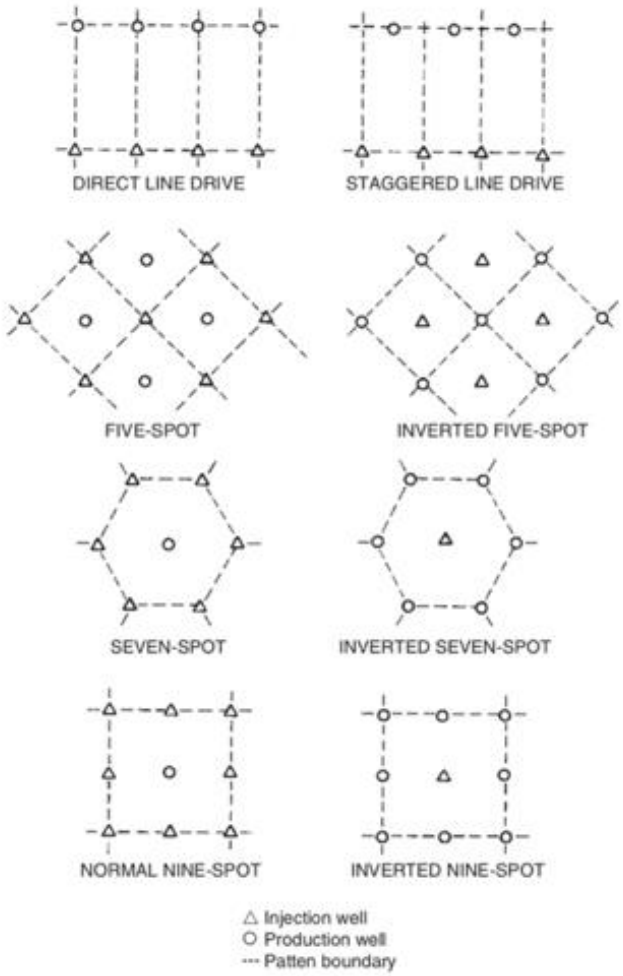

Figure 2 Pattern Injection Schemes [12]

3. Peripheral Injection: the injector wells are placed on the outskirts of the reservoir as shown in Figure 3.

   In peripheral injection, sufficient permeability is required in order to allow the fluid being injected to move at an acceptable rate towards the center of the field where the producers are located since the injectors are placed around the periphery of the producers [16]. Ahmed [16] also discussed that there will be a delay in the field response to the fluid being injected as it takes time for the injected fluid to reach the different parts of the reservoir. He also stated that, in order to prevent the injection fluid from bypassing any movable oil, the

producers that have been watered-out may be converted into injectors, and so significant water production quantities can be delayed until the last row of producers remains.

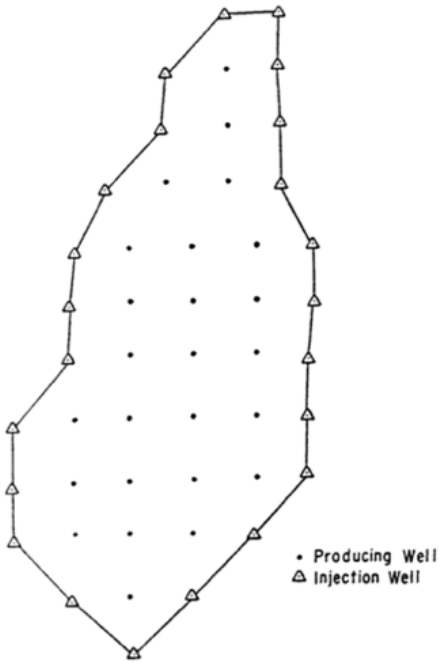

Figure 3 Peripheral Injection Scheme [16]

4. Crestal and Basal Injection: In crestal injection, the injector wells are placed at the top of reservoirs that have sharp structural features (gas caps). This injection scheme is mainly used for gas injection [16]. In basal injection, the injector wells are positioned down dip and the fluid is, as seen in Figure 4, injected at the bottom of the structure. Basel injection patterns are used in many water injection projects to take advantage, and benefit from gravity segregation [17].

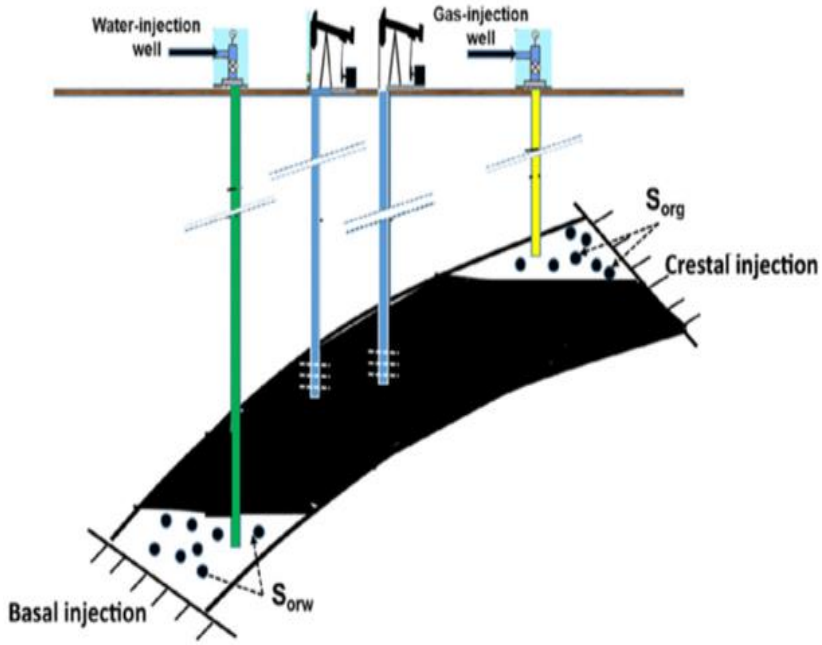

Figure 4 Crestal and Basal Injection Schemes [16]

1.2.3. Water Injection Efficiency Challenges

Factors affecting sweep efficiencies that must be considered when placing injector wells are: (1) reservoir heterogeneity including high permeability streaks, faults and fractures, (2) free water levels, (3) availability of the fluid being injected (gas or water), (4) distance between the wells known as well spacing, (5) adequate fluid injection rates so that the desired production rate is obtained, and (6) maximizing the recovery of the oil/gas while minimizing production of injected fluid [16].

In a case study conducted by Satter et al. [17] on a field located in the Northern American continent, low oil recovery using water injection was attributed to low formation permeability, to the absence of perforations in specific pay zones, and to the channeling of injected water due to fracturing. In another study, Bibars [15] discusses the injection challenges faced when producing from the El Morgan Kareem reservoir located in the Gulf of Suez. Bibars [15] observed unexpected high-water production which was mainly caused by one of the 8 zones (Zone 2) present in the reservoir. After

carrying out several studies, it was discovered that the water injected yielded an uneven distribution profile in Zone 2 due to its high permeability. This led to the bypassing of the oil, by the injected water, in the deeper zones, and almost 80% of the injection rates were received by this zone. Similarly, the Spring Field demonstrated an uneven water distribution profile caused by a complex reservoir structure [18]. Moreover, a multi-layered, highly heterogeneous reservoir located in the Sabriyah Field of North Kuwait called the Upper Burgan reservoir encountered injectivity complications associated with severe faulting and compartmentalization. The compartments were found to have varying oil/water contacts, aquifer support, and reservoir pressure [19].

1.2.4. Peripheral Water Injection Scheme Case Studies

As highlighted previously, the importance of water injection is to prevent rapid pressure decline with time, by providing pressure support to the reservoir, in order to enhance the displacement of oil [20]. Additionally, the type of injection scheme employed is highly influenced by the characteristics of the reservoir [21]. In some reservoirs, it is inefficient to employ a line-drive or 5-spot patterns; while in others, peripheral cannot be used.

1.2.4.1. Case Study 1

A study by Guari et al. [22] focused on the improvement made by ADNOC Offshore to a field development plan of one of its reservoirs. Based on the initial reservoir model a 5 – spot water injection scheme was selected. The injection scheme was selected based on testing several field development scenarios in which, due to low transmissibility, peripheral water injection showed no added value when compared to

natural depletion. Accordingly, 5-spot water injection was adopted. During initial production, it was found that the formation transmissibility (KH) ranged between 300-5300 md. ft, however, further data acquisition was carried out showing transmissibility values that are 10 times higher in the crestal region of the reservoir [22]. The mismatch of results brought forth further testing as the 5-spot injection was no longer valid.

Guari et al. [22] then revisited the possibility of implementing peripheral injection schemes for several reasons including (1) mitigating risk of early water breakthrough, (2) efficient uniform sweep, (3) high connectivity in the reservoir, (4) low bubble point pressure, and (5) water cycling risk due to differential depletion. It was also mentioned that a 5-spot water injection scheme, due to reasons (3) & (4), would risk water breakthrough and lower recovery from layers that have poor reservoir characteristics [22]. Peripheral water injection was then compared to 5-spot pattern water injection, on an updated simulation model, in which the main difference between the development plans was the conversion of the injectors to producers, in the oil pool, in the case of peripheral injection.

The peripheral injection results obtained showed an increased plateau length and reduced water cut which is representative of effective sweep and less water cycling. Despite the outcome, the saturation map uncovered a fair amount of upswept oil in the center part of the reservoir, and a semi-peripheral water injection scheme was employed to overcome this drawback. So, 4 injectors were placed in the center of the reservoir, and a further reduction in the water cut was observed compared to peripheral water injection. The ‘increased injectors with reduced water cut’ phenomena was a result of the better pressure support the reservoir was receiving in the middle, whereas, in the

case of peripheral injection, the injectors needed to inject larger volumes of water to maintain the pressure in the reservoir [22].

1.2.4.2. Case Study 2

The layered and extremely faulted carbonate Mauddud reservoir located in the Gulf Region has been dominated by a crestal gas injection recovery mechanism since 1938 [23]. In 2011, a 5-spot injection scheme was proposed and implemented leading to a premature water breakthrough in most of the producers (mainly the producer located in the center) [23]. The outcome of using 5-spot injection in a reservoir that is comprised of high permeability vugs and layers was deficient sweep and water cycling [23]. In 2013, the pattern injection scheme was converted into a peripheral injection scheme by turning the water injectors in the center into producers. Hence, this realignment reduced water cut and impeded production decline [23].

1.2.4.3. Case Study 3

Yadav et al. [24] carried out a study on a mature offshore oil field located in the Gulf of Suez. The field, first discovered in 1977, was composed of a very complex structure. The faults in the reservoirs severely disturbed the field structure dividing it into 42 compartments. The primary source of recovery of oil is attributed to bottom aquifer support, that is later followed by peripheral water injection as a secondary source of recovery [24]. Once water injection began, some layers started to water-out due to the reservoir's heterogeneities and variable pressure across the different layers, leading to a decline in field production. However, early water breakthrough mainly occurred in the reservoir units whose vertical communication of flow was blocked by

the presence of horizontal shale barriers [24]. Also, as the field constitutes of many layers, the wells that were producing from the reservoir units present at the bottom of the field produced unreasonable amounts of water that was coming from the injection wells or aquifer. Reasons for the aforementioned situation were associated with, again, the reservoir's heterogeneities and higher vertical permeability. Hence, this led Yadav et al. [24] to conclude that the application of peripheral water injection added to an aquifer filled reservoir with a faulted and complex structure results in poor vertical and areal sweep efficiencies.

It can be noticed that different reservoirs face varying challenges. Satter [17] states that these challenges require an integrated team approach that is equipped with a detailed and accurate reservoir description. Furthermore, past reservoir performance needs to be monitored and interpreted, laboratory analysis needs to be carried out, and reservoir models need to be validated and developed. Injection schemes and their implementation are critically dependent on a reservoir surveillance program that must be developed prior to any project [17]. Reservoir surveillance programs include field development planning, reservoir pressure measurement, static and dynamic reservoir model updates, pressure transient tests, monitoring well rates and bottom hole pressure, water injection rate control, etc [17].

1.3. Particle Swarm Optimization

One of the most commonly used optimization techniques, nowadays, is particle swarm optimization [25]. PSO is an algorithm that resembles schools of fish or flocks of flying birds. The 'swarm' represents a group of particles, and the position of each 'particle' represents a solution of the objective function [26]. Initially, the particles are

assigned random positions and velocities, and then the particles position in the search space is updated depending on a calculated velocity parameter [26]. The individuals or particles in this optimizer evolve by competing and cooperating among themselves through the entire process. The direction in which each particle in the swarm takes to fly is adjusted according to the particles own flying experiences and to the other particles' flying experiences. Each particle represents a possible solution to a problem [26]. Furthermore, since PSO was presented in 1995 it has undergone many enhancements. Over time, as researchers familiarized themselves with the algorithm, they derived new versions of PSO, developed new implementations of it in a multitude of areas, and issued theoretical studies that aimed at exploring the effects that its various algorithmic parameters have [27]. Moreover, the computational behavior of a workflow is significantly affected by these parameters. In other words, with some settings it may uncover desirable computational behavior, while with others, it may not, and so, algorithmic parameter selection is of high importance [25]. These algorithmic parameters are often referred to as the exploration-exploitation tradeoff in which "exploration is the ability to test various regions in the problem space in order to locate a good optimum, hopefully the global one, while exploitation is the ability to concentrate the search around a promising candidate solution in order to locate the optimum precisely", as defined by Trelea [28]. However, the parameter selection process for the algorithm remains empirical to a large extent despite recent research efforts [28].

1.3.1. Algorithmic Parameters

PSO has several appealing advantages including it being an easy to implement algorithm, and also having but few parameters to adjust [29]. These parameters include inertia weight (w), learning factors ($c_g \ and \ c_p$), swarm size and stopping criteria [27]. Many studies were conducted in which researchers study the influence of a single parameter and fix the other parameters, while other researchers have accessed the effect of multiple parameters at the same time [27].

1.3.1.1. Inertia Weight

One of the key parameters in PSO is the Inertia Weight (w), however, this parameter was not introduced to PSO until 1998 by Shi and Eberhart [26]. The Inertia Weight determines how much of the previous particle's velocity will contribute to the current particle's velocity thereby bringing about a balance between the exploitation and exploration abilities of PSO and enhancing convergence [30,31].The aforementioned advantages lead to the requirement of fewer iterations to find the optimum if the Inertia Weight is suitably selected [33]. Since the adoption of this parameter there have been proposals of several strategies for determining its value [29,30], yet Gubta and Choubey [32] stated that the four best Inertia Weight techniques that have been introduced over the years are: Constant Inertia Weight (CIW), Linearly Decreasing Inertia Weight (LDIW), Global-Local Best Inertia Weight (GLBIW), and Chaotic Decreasing Inertia Weight (CDIW) [32]. In the following paragraphs, a review of the previously mentioned Inertia Weight strategies is given.

As previously mentioned, the basic PSO algorithm that was presented in 1995 by Eberhart and Kennedy [33] has no Inertia Weight [33]. Nonetheless, the concept of

Inertia Weight was introduced for the first time by Shi and Eberhart in 1998 in which they proposed a CIW strategy. They tested their proposed strategy on Schaffer's f6 function in order to see the impact in which the inertia weight has on the performance of PSO. Moreover, this function was adopted because its global optimum is known. It should be noted that, for the purpose of comparison, all the simulations carried out had the same PSO settings except the inertia weights. Shi and Eberhart assessed a range of constant inertia weights for simulation including $w = 0$, 0.8, 0.85, 0.9, 0.95, 1, 1.05, 1.1, 1.2, and 1.4, and used a swarm size of 20 particles [26].

Shi and Eberhart [26] reasoned that PSO is identical to a local search algorithm for inertia weight values less than 0.8. However, they stated that if an acceptable solution exists within the initial search space, then the global optimum can be found by PSO quickly, else it will not find the global optimum. On the other hand, for inertia weight values larger than 1.2, PSO is identical to a global search method. It was reported by Shi and Eberhart [26] that larger inertia weight values are not very dependent on initial search space solutions, and so PSO would be more capable of exploring new areas. In other words, smaller inertia weights tend to promote local exploitation while larger inertia weights facilitate global exploration [26]. It was concluded that PSO with a constant inertia weight value between 0.9 and 1.2, on average, performs better and has a higher probability of finding the global optimum [26].

In general, Shi and Eberhart [26] deduced, for any optimization search algorithm, that the algorithm would be better off at the beginning to exhibit an exploration ability in order to find a good seed, and then exhibit a more exploitation ability to fine tune the local area around the seed [26]. Based on the previous deduction,

Shi and Eberhart [26] brought about an inertia weight function that linearly decreases as a function of time. This function is listed in Table 1. They tested it within an inertia weight range of 1.4 to 0 and, compared to previous results of constant inertia weight values, it showed significant improvement of PSO performance. The authors brought their study to an end by suggesting that further studies need to be carried out in order to test and see whether a more suitable LDIW range can be found [26].

Later that year, Shi and Eberhart [34] built on their previous study of the LDIW and were able to provide guidelines for selecting the inertia weight parameter. They carried out many experiments using the same function (Schaffer's f6 function) and the same settings as their preceding paper. Shi and Eberhart [34] found that experimentally a LDIW from 0.9 to 0.4 yields excellent results. Shi and Eberhart [35] then extensively investigated the PSO performance with a LDIW from 0.9 to 0.4 by testing on several benchmark functions including the Sphere, Rosenbrock, Rastrigin, and Griewank functions. Also, swarm sizes of 20, 40, 80, and 160 particles were used. It was reported, for all testing cases, that the PSO algorithm was able to converge swiftly, however, towards the end of a run, it lacked global search abilities [35]. Nevertheless, results illustrate that by using a LDIW, the performance of PSO was improved greatly and displayed better results than that of a CIW.

In 2006, Arumugam and Rao [36] proposed a new inertia weight called the Global-Local Best Inertia Weight (GLBIW), listed in Table 1. This strategy is neither set as a linearly decreasing function, nor set to a constant value [36], instead it is a function of the global and local best values, for each iteration, of the objective function. [36]. Arumugam and Rao [36] stated that the suggested strategy improves the performance of PSO in terms of both faster convergence and solving high dimensional

problems. Furthermore, in 2010, Umapathy, Venkataseshaiah, and Arumugam [37] considered testing a CIW, a LDIW, and a GLBIW on a standard IEEE 30 bus test system in order to analyze the impact of the three listed inertia weight strategies on the PSO performance. The results obtained showed that GLBIW outperformed CIW and LDIW in terms of the performance of PSO and resulted in fast convergence, consistency, high quality solutions, and an algorithm that is computationally faster [37].

In 2007, Feng et al. [38] presented a chaotic decreasing inertia weight (CDIW) strategy that was based on the LDIW. Like Shi and Eberhart [26,35], Feng et al. [38] investigated the effect of a CDIW, from 0.9 to 0.4, on the performance of PSO, by testing on several benchmark functions including the Sphere, Rosenbrock, Rastrigin, Griewank, and Schauffer f6 functions. Moreover, all their experiments were carried out using a swarm size of 20 particles. Feng et al. [38] indicated the following outcomes of a CDIW strategy: an increase in the optimum fitness result, a preferable convergence precision, stability, robustness, and better global search ability. It was also noted by the authors that the particles were able to move out of a local optimum, when stuck, and search for the global optimum result [38].

Table 1 Inertia Weight Formulas

Name of Inertia Weight	Formula of Inertia Weight	Reference
Constant Inertia Weight	$w = c$	[31]
Linearly Decreasing Inertia Weight	$w = (w_{max} - w_{min}) \frac{Iter_{max} - Iter_{\ current}}{Iter_{max}} + w_{min}$	[39]
Global-Local Best Inertia Weight	$w = 1.1 - \frac{gbest}{pbest}$	[36]
Chaotic Decreasing Inertia Weight	$w = (w_{max} - w_{min}) \frac{Iter_{max} - Iter_{\ min}}{Iter_{max}} + w_{min} z$ $z = 4z(1 - z)$	[38]

1.3.1.2. Acceleration Coefficients

The acceleration coefficients, $c_g \ and \ c_p$, represent the weight in which a particle is being pulled towards its best global optima and best local optima, respectively, across the iterations carried out in a certain workflow [25,27]. The risk of the particles getting trapped in false optima rises when the value of these constants is too high due to the abrupt movement of the particles. On the contrary, very low values of the acceleration constants would result in slow movement of the particles and lead to a significant increase in computational effort [25]. Moreover, it should be noted that when the value of the cognitive acceleration coefficient (c_p) increases, the particles attraction towards the local best optima is enhanced while its attraction towards the global best optima is decreased. Conversely, when the value of the social acceleration coefficient (c_g) increases, the particles attraction towards the global best optima is enhanced while its attraction towards the local best optima is decreased [25].

The acceleration factors, in many cases in literature, are set to 2.0 since for most problems this a commonly acceptable setting and is also extensively used in practical PSO applications [25,27]. The value 1.49445 is another common value used [27]. In 2001, Carlisle and Dozier [40] suggested in their work that it is favorable to adjust the cognitive/social ratio to lean towards the cognitive acceleration coefficient. After many experimentations, Carlisle and Dozier [40] reported that $c_p = 2.8 \; and \; c_g = 1.3$ returned the best performance, which was later confirmed by Schutte and Groenwold [40]. Other researchers were inspired by the linearly decreasing inertia weight strategy and implemented it on the acceleration factors, while others experimented with trial and error to find values that would best fit their work [25,27]. Overall, in most settings, the two acceleration coefficients $c_g \; and \; c_p$ have equal values for the purpose of a same weight social and cognitive search [27].

1.3.1.3. Swarm Size and Stopping/Convergence Criteria

The swarm size, which is the number of particles used for a certain workflow, significantly affects the performance of PSO [25]. In most cases, using an increased number of particles decreases the number of required algorithmic iterations since the particles would be sampling the search space more thoroughly, however the function evaluation requirements would increase and slow down the algorithm [25,28]. On the other hand, using too few particles would result in the algorithm getting trapped in a local optimum, hence decreasing reliability. Usually a swarm size of 20-30 particles would be a rational trade-off between cost and reliability, however, in literature, there is no precise rule for swarm size selection besides the fact that when the complexity of the problem increases, in general, so should the swarm size [25,27,41].

1.3.1.4. Convergence Criteria

Similarly, the convergence/stopping criteria also depend on the problem at hand. It can be that a prescribed number of iterations is reached, a specified quality in the solution is obtained, a passing of a specified time limit, a lack of deviation in particular sequential iterations or a combination thereof [25].

1.3.2. PSO in Well Placement Optimization

Many researchers have employed PSO in well placement optimization problems. The table below summarizes the different well placement optimization studies that have used PSO, over the years, with the combination of algorithmic parameters that they used. It can be seen from

Table 2 that the use of a CIW of 0.721, and acceleration factors equivalent to 0.193 is very common among researchers in the field of well placement optimization. These values were determined by Clerc [42] from numerical experimentation, however, can be optimized [8].

Table 2 PSO in Well Placement Optimization

Title	Inertia Weight	Acceleration Factor	Swarm Size	Reference
Black hole particle swarm optimization for well placement optimization	$w = 0.721$ (CIW)	$c_g = c_p = 1.193$	10,15,20	[1]

A New Well-Pattern-Optimization Procedure for Large-Scale Field Development	$w = 0.721$ (CIW)	$c_g = c_p =$ 1.193	20,40	[8]
Efficient well placement optimization coupling hybrid objective function with particle swarm optimization algorithm	$w = 0.721$ (CIW)	$c_g = c_p =$ 1.193	50	[43]
Optimization of Well Placement by PSO Assisted by Quality Map and Gompertz-Based Grey Model	$w = 0.721$ (CIW)	$c_g =$ c_p =1.193	50	[44]
Application of a particle swarm optimization algorithm for determining optimum well location and type	$w = 0.721$ (CIW)	$c_g =$ c_p =1.193	5,10,20,30,40	[45]
Well placement optimization using metaheuristic bat algorithm	w_{min} $= 0.4$ w_{max} $= 0.9$ (LDIW)	$c_g =$ c_p =0.775	25	[46]
Well placement optimization subject to realistic field development constraints	[$w_{min} =$ 0 $w_{max} = 1.2$ (LDIW)	c_g =1.2, $c_p =$ 1.2	25	[47]

Hybrid differential evolution and particle swarm optimization for optimal well placement	$w = 0.721$ (CIW)	$c_g =$ $c_p =1.193$	5,10,20	[48]

1.4. Study Objective

In a recent work by Harb et al. [1], the black hole particle swarm optimization (BHPSO) was introduced. It is a new hybrid evolutionary optimization method that simultaneously and systematically optimizes the well count, location, type, and trajectory in a field development plan. The proposed method was implemented and tested on the Olympus Challenge focusing on well placement in a pattern water injection scheme.

However, the work did not address the case of peripheral water injection schemes which might be a more suitable development scenario depending on the type of field under study. The work also didn't define a clear convergence criterion for the algorithm which is very critical considering the small-time window for decisions. Hence, we focus in this thesis on expending the applicability and improving the performance of BHPSO through:

1. Implementing Peripheral Injection scheme in the BHPSO workflow (verified throughout the course of this work)
2. Testing and evaluating different black holing techniques
3. Defining a convergence criterion for BHPSO optimization workflow

CHAPTER 2

FIELD DESCRIPTION

In this work, the algorithm was tested on two synthetic oil fields for well placement optimization: Olympus and PUNQ-S3. A description of both fields is presented in this chapter.

2.1. Olympus

Olympus is a synthetic reservoir model developed by TNO for the purpose of a benchmark study for field development optimization [49, 50]. It has 342,000 grid blocks of which 192,750 blocks are active and is 50 m thick for which 16 layers have been modeled [50]. Due to being separated by an impermeable shale layer, the reservoir is made up of an upper zone and a lower zone [49]. The upper reservoir zone is made up of channel sands, as can be seen in Figure 6, lodged in floodplain shales, while alternative layers of coarse, medium, and fine sands make up the lower reservoir zone [50].

50 subsurface realizations where generated for the Olympus field to cover uncertainty in reservoir properties. In these realizations, the grid, faults, and OWC are kept unchanged, while the porosity, permeability, NTG, and initial water saturation vary. The field, on one side, is bounded by a sealing fault while 6 other minor faults exist in the reservoir [50]. Moreover, the Olympus is a 2-phase model: oil and water. Harb et al. [1] tested well placement in a pattern water injection scheme on Olympus

Upper, Realization 22 (U22) and Olympus Lower, Realization 6 (L6). In this study, the U22 is used.

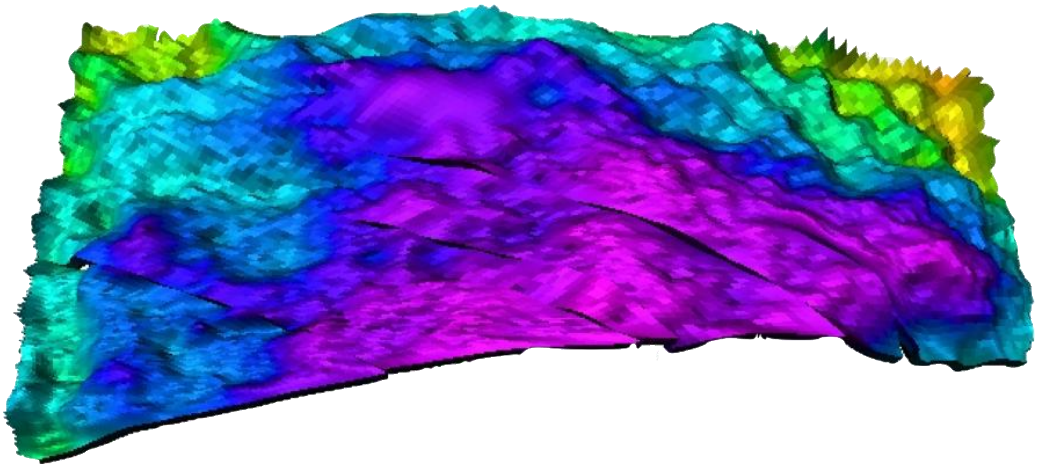

Figure 5 Olympus three-dimensional reservoir model. The field shows initial reservoir pressure for the Upper 22 realization. Purple, blue and green represent approximately 200 bars, 206 bars, and 215 bars, respectively

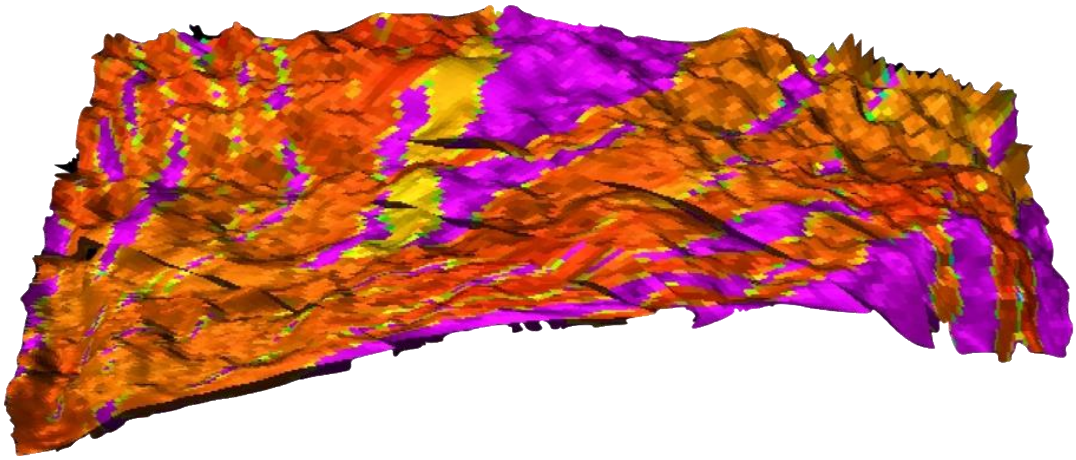

Figure 6 The 3D field shows horizontal permeability for the Upper 22 realization. Orange, yellow and pink represent approximately 1000 mD, 100 mD, and 0, respectively

2.2. PUNQ-S3

PUNQ-S3 is a small-size synthetic reservoir model based on a real field operated by Elf Exploration Production [46,51,52]. It has 2660 grid blocks of which 1761 blocks are active and is approximately 28 m thick [46]. The 2-phase model of oil

and water has an average reservoir porosity of 0.2, and an average horizontal permeability of 100 mD. To the east and south, the field is bounded by faults, while to the north and west it is linked to a fairly strong aquifer [46].

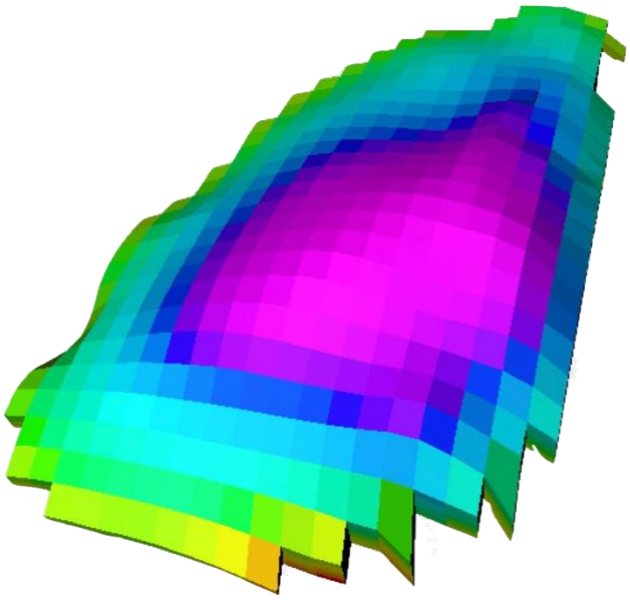

Figure 7: PUNQ-S3 three-dimensional reservoir model. The field shows initial reservoir pressure. Pink, blue and green represent approximately 234 bars, 236 bars, and 238 bars, respectively

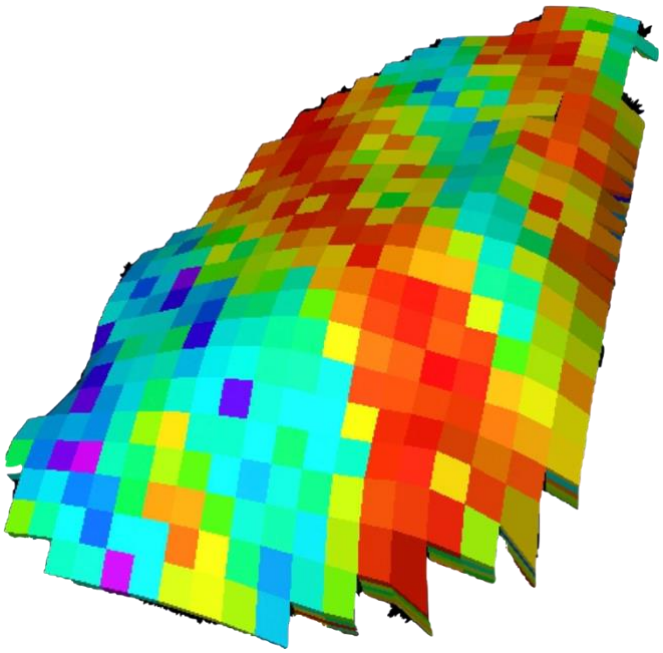

Figure 8: The 3D field shows horizontal permeability for the PUNQ-S3 field. Orange/red, yellow/green and pink represent approximately 1000 mD, 100 mD, and 0, respectively

2.3. Objective Function

In this work, the objective function to be optimized is the net present value (NPV) and is evaluated over a fixed project period of 20 years. In Table 3, the input parameters that are needed to calculate the objective function are listed.

The NPV is calculated, in US dollars, as follows:

$$NPV = \sum_{i=1}^{N_t} \frac{R(t_i) \times \Delta t_i}{(1+d)^{t_i/\tau}} \quad (1)$$

where, d is the discount factor, $\Delta t_i = t_i - t_{i-1}$ is the time period, in days, between t_i and t_{i-1}, τ is the number of days in a year, and $R(t_i)$ is the sum of all expenses and incomes earned within the time period Δt_i. The cost term $R(t_i)$, in US $, is calculated as follows:

$$R(t_i) = Q_{op}(t_i) \times rop - Q_{wp}(t_i) \times rwp - Q_{wi}(t_i) \times rwi - P - D(t_i) \quad (2)$$

where, Q_{op} is the cumulative oil production volume over Δt_i, Q_{wp} is the cumulative water production volume over Δt_i, and Q_{wi} is the cumulative water injection production volume over Δt_i. Rop is the oil revenue (price), rwp is the water production cost, and rwi is the water injection cost (all in $/unit volume). P is the platform cost, and $D(t_i)$ is the total drilling and completion costs acquired across the Δt_i time period.

Table 3 Input parameters needed to calculate the objective function

Contribution	Cost	Units
Platform Cost	500	Million $
Oil Price	45	$/bbl
Water Production Cost	6	$/bbl
Water Injection Cost	2	$/bbl
Annual Discount Factor	0.08	Dimensionless

CHAPTER 3

METHODOLOGY

The BHPSO algorithm combines two algorithms: (1) the particle swarm optimization algorithm (PSO) and (2) the black hole operator (BHO). Both algorithms will be described in this section before detailing the approach through which they were combined to form the BHPSO. However, the BHO and BHPSO will be described through a peripheral injection scheme scenario; the subject of this study. Also, changes and improvements for the overall workflow will be highlighted through this scheme.

3.1. PSO – Particle Swarm Optimization

The PSO algorithm, inspired by the behavior of flocks of birds and schools of fish, was developed by Kennedy and Eberhart in 1995 [33]. It is a population based stochastic search method that is a member of the swarm intelligence techniques class [33]. In the optimization workflow, the 'swarm' represents a group of particles, and the position of each 'particle' represents a solution of the objective function [1,33]. Initially, the particles are assigned random positions and velocities, then the objective function values are calculated for all the particles. The particles position, in the search space, is then updated depending on a calculated velocity parameter [33]. Using a mathematical formulation, the velocity parameter is calculated based on the particle's velocity from the previous iteration, the particles distance from the position where it achieved its local best, and the particles distance from the particle that achieved the global best [1]. In each iteration, the algorithm memorizes the particles' best position/solution known as the local best position and the swarms overall best

position/solution known as the global best position [1]. Moreover, the objective function is calculated at each iteration for each particle. The velocity and positions are calculated as follows:

$$v_{i,j}(k+1) = w \times v_{i,j}(k) + c_p r_1 \left(p_{best\,(i,j)} - x_{i,j}(k)\right) + c_g r_2 \left(g_{best\,(i,j)} - x_{i,j}(k)\right) \quad (3)$$

$$x_{i,j}(k+1) = x_{i,j}(k) + v_{i,j}(k+1) \quad (4)$$

where i, j, and k refer to the particle, the optimization variable, and the current iteration respectively. The three main parameters involved in the velocity equation are: the cognitive weight (c_p), the social weight (c_g), and the inertia weight (w). The influence of the trend toward the particle's previous velocity is defined by the inertia weight, as the influence of the trend toward the particles local best position is defined by the cognitive weight. As for the social weight, it is defined by its effect on the trend toward the swarm's global best position [1]. Note that r_1 and r_2 are two independent random variables between 0 and 1. In this work, the star PSO is employed with algorithmic parameters of $w = 0.721, c_p = c_g = 1.1931$, however by conducting a sensitivity analysis on the algorithmic parameters c_p, c_g, and w the PSO convergence rate can be assessed [1]. The PSO mathematical formulation is demonstrated below:

Iteration 1:

1. Initialize the particles with random positions and velocities
2. Calculate f(x) for each particle
3. Set $p_{best(ij)} = x_{ij}$ for each particle
4. Set $g_{best(ij)} = x_{ij}$ of $f(x)_{max}$

Iteration k+1:

5. Calculate v_{ij} for each particle using equation 3
6. Calculate x_{ij} for each particle using equation 4
7. Calculate $f(x)$ for each particle
8. Select local best by finding the maximum value of $f(x)$ between the current and previous iteration for each particle independently. For the 1st particle, if $f(x_1)_{iteration1} > f(x_1)_{iteration2}$ then $p_{best(11)iteration2} = p_{best(11)iteration1}$ and $p_{best(12)iteration2} = p_{best(12)iteration1}$, else the local best of the current iteration will be the position values obtained in the current iteration.
9. Select global best by finding the maximum value of $f(x)$ between the current and previous iteration and setting $g_{best(ij)} = x_{ij}$ of $f(x)_{max}$.
10. Repeat steps 5-9 until maximum number of iterations is reached, or convergence is reached.

Table 4 Mathematical formulation of PSO given two decision variables

$Particle\ Number$	$v(velocity)$		$x(position)$		$f(x)$	p_{best} $(local\ best)$		g_{best} $(global\ best)$	
	DV_1	DV_2	DV_1	DV_2		DV_1	DV_2	DV_1	DV_2
1	v_{11}	v_{12}	x_{11}	x_{12}	$f(x_1)$	$p_{best(11)}$	$p_{best(12)}$		
2	v_{21}	v_{22}	x_{21}	x_{22}	$f(x_2)$	$p_{best(21)}$	$p_{best(22)}$	[…,…]	
3	v_{31}	v_{32}	x_{31}	x_{32}	$f(x_3)$	$p_{best(31)}$	$p_{best(32)}$		

In the final part of this study, the effect of a Linearly Decreasing Inertia Weight on PSO performance was studied including a sensitivity analysis on the acceleration

coefficients, c_p and c_g. The Linearly Decreasing Inertia Weight (LDIW) is calculated as follows:

$$w_{LDIW} = (w_{max} - w_{min}) \frac{Iteration_{max} - Iteration_{current}}{Iteration_{max}} + w_{min} \quad (5)$$

$$v_{i,j}(k+1) = w_{LDIW} \times v_{i,j}(k) + c_p r_1 \left(p_{best\ (i,j)} - x_{i,j}(k)\right) + c_g r_2 \left(g_{best\ (i,j)} - x_{i,j}(k)\right) \quad (6)$$

where w_{max} and w_{min} are 0.9 and 0.4 respectively, and $Iteration_{max}$ is the maximum number of allowed iterations. The PSO mathematical formulation, for a LDIW strategy, is demonstrated below:

Iteration 1:

1. Initialize the particles with random positions and velocities
2. Calculate f(x) for each particle
3. Set $p_{best(ij)} = x_{ij}$ for each particle
4. Set $g_{best(ij)} = x_{ij}$ of $f(x)_{max}$

Iteration k+1:

5. Update the inertia weight value using equation 5
6. Calculate v_{ij} for each particle using equation 6
7. Calculate x_{ij} for each particle using equation 4
8. Calculate $f(x)$ for each particle
9. Select local best by finding the maximum value of $f(x)$ between the current and previous iteration for each particle independently. For the 1st particle, if $f(x_1)_{iteration1} > f(x_1)_{iteration2}$ then $p_{best(11)iteration2} = p_{best(11)iteration1}$ and $p_{best(12)iteration2} = p_{best(12)iteration1}$, else the local best of the current iteration will be the position values obtained in the current iteration.

10. Select global best by finding the maximum value of $f(x)$ between the current and previous iteration and setting $g_{best(ij)} = x_{ij}$ of $f(x)_{max}$.
11. Repeat steps 5-10 until maximum number of iterations is reached, or convergence is reached.

3.2. Black Hole Operator for Well Placement Optimization in a Peripheral Water Injection Scheme

The black hole operator is an algorithm responsible for the generation of ready to be used well trajectories, mainly for reservoir simulation purposes. The main quality maps used for well placement, the different black holing techniques, and the input parameters to the algorithm will all be described in the sections below.

3.2.1. Maps

3.2.1.1. Net Hydrocarbon Thickness Map

The Net Hydrocarbon Thickness map (NHCT) is the main quality map used for producer placement and is an indication of hydrocarbon "sweet" spots in different parts of the reservoir. The NHCT map is a version of a map that reflects condensed reservoir properties including hydrocarbons initially in place, porosity, and permeability. For a 3D reservoir simulation model with i and j coordinates, the NHCT is calculated as follows for a cell in the aerial direction [1]:

$$NHCT_{ij} = \sum_{k=1}^{N_k} \varphi_{ijk} NTG_{ijk} \left(1 - S_{w_{ijk}}\right) Z_{ijk} \tag{7}$$

where $\varphi_{ijk}, NTG_{ijk}, S_{w_{ijk}}$, and Z_{ijk} indicate the porosity, net-to-gross, water saturation, and thickness of the grid block cell ijk, respectively [1]. The unit of $NHCT_{ij}$ is the same as that of Z_{ijk} which is in meters (feet) since φ_{ijk}, NTG_{ijk}, and $S_{w_{ijk}}$ are dimensionless. An example of a NHCT map is depicted in Figure 9 and Figure 12. The yellow colour represents high NHCT, while the purple colour is an indication of areas completely saturated with water (no oil). Typically, the yellow regions would be the best location to place a producer.

3.2.1.2. "Kh" Map

For a pattern injection scheme, the NHCT map is ideal for both producer and injector placement, however for a peripheral injection scheme the 'Kh' map is more suited for the placement of injectors [1]. Where the NHCT map is an indication of the hydrocarbon thickness, the Kh map is an indication of the permeability thickness. The 'Kh' Map is the quality map used for the placement of injectors in a peripheral injection scheme. It is an indication of permeability "sweet" spots. For a 3D reservoir simulation model with i and j coordinates, the Kh is calculated as follows for a cell in the aerial direction:

$$Kh_{ij} = \sum_{k=1}^{N_k} k_{ijk} Z_{ijk} \tag{8}$$

where k_{ijk} denotes the (aerial) permeability of grid block cell ijk [1]. The Kh map depicts the outskirts of the reservoir and is dictated by a "ring" through which injectors will be placed (See Figure 10 and Figure 13). The yellow colour represents high permeability, while the purple colour is an indication of areas of low permeability. Typically, the yellow regions would be the best location to place an injector.

3.2.1.3. Horizon Map

A structured map known as the Horizon map is a representation of the depth that the horizontal section length of a well can be placed in. A reservoir is made up of several horizons, and so, in a sensitivity analysis, the horizon that contains the highest volume of hydrocarbons initially in place, can be selected to place the well length in.

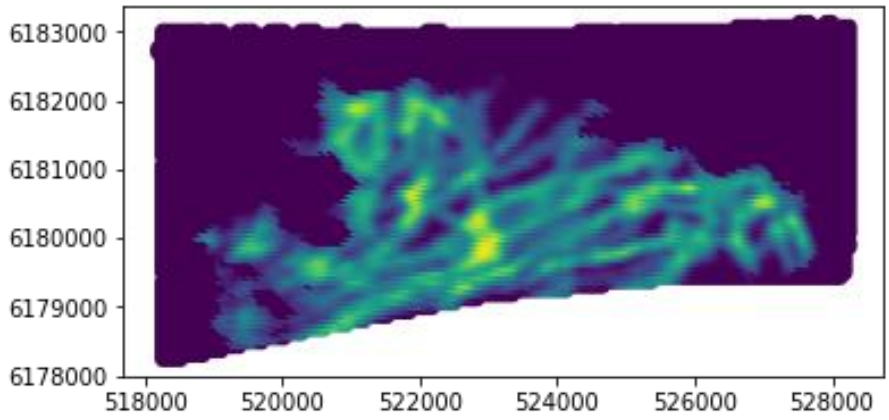

Figure 9 Net Hydrocarbon Thickness Map – U22

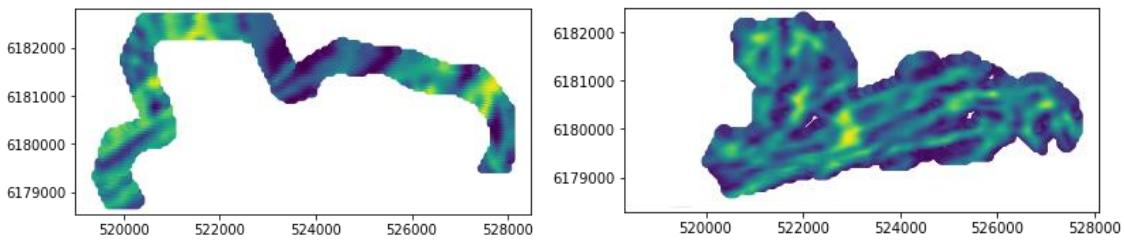

Figure 10 Kh map (Left) and NHCT map (Right) used for well placement in a peripheral water injection scheme – U22

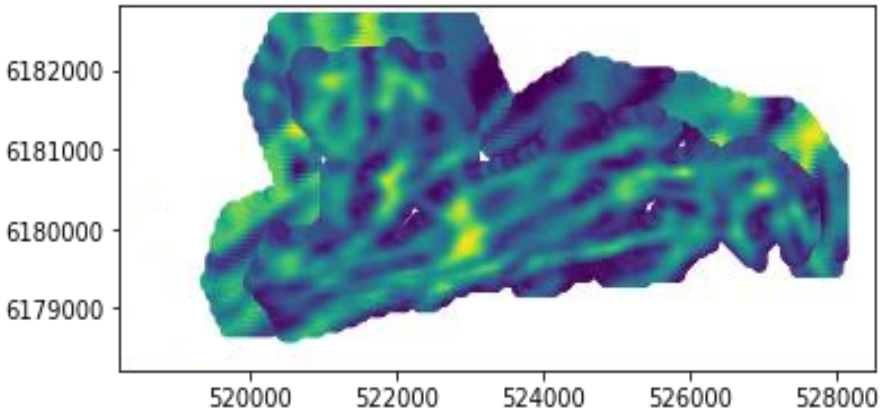

Figure 11 Illustration of the "Combined" set of two maps: NHCT map and Kh map used for well placement in a peripheral water injection scheme – U22

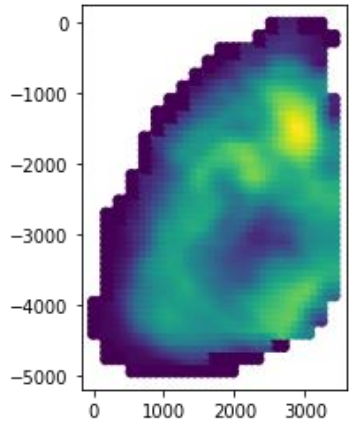

Figure 12 Net Hydrocarbon Thickness Map – PUNQ-S3

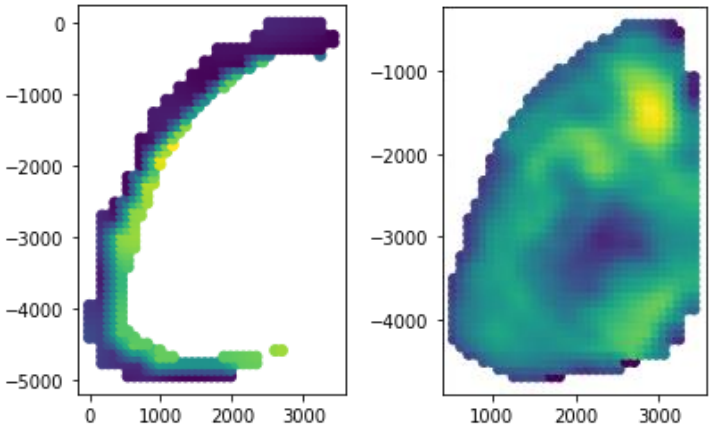

Figure 13 Kh map (Left) and NHCT map (Right) used for well placement in a peripheral water injection scheme – PUNQ-S3

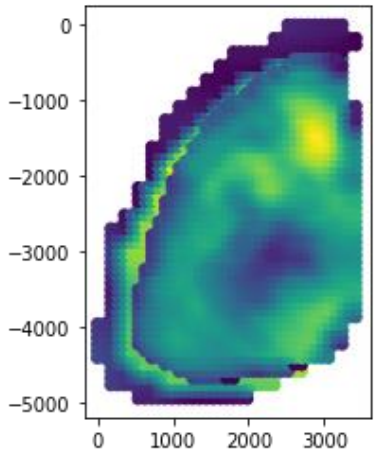

Figure 14 Illustration of the "Combined" set of two maps: NHCT map and Kh map used for well placement in a peripheral water injection scheme – PUNQ-S3

3.2.2. Black Holing Techniques: Point vs Region

In a pattern water injection scheme, when placing wells, the black hole operator searches for the highest NHCT points on the map. The first wells heel/toe is placed at this point, and the algorithm goes on to search for the second highest NHCT point to place the second well, and so on. However, with the introduction of a peripheral injection scheme, a region search option was introduced to the algorithm. This region search option was proposed in order to place the injectors based on high permeability regions, on the KH map, instead of high permeability points.

The region search option, known as the Radius Optimal Option, works as follows: (1) A radius optimal value (ROV) is given to the region search option in the algorithm, which (2) searches for high property regions specific to the map, i.e. permeability, NHCT. This search space is defined by a disk with a radius given by the ROV. For example, given a ROV of 150 m, the algorithm will take each point on the map and create a disk around it with the given radius, as can be seen in the figures below. (3) The algorithm will then sum up the value of the points within the disk and

seek out the disk that returns the highest property value. (4) The first well will be placed in the center of this region/disk, and then (5) the algorithm will seek out the disk that returns the second highest property value and place the second well there, and so on. For example, in Figure 15, the algorithm will return summed up permeability values, whereas in Figure 16, the algorithm will return summed up NHCT values. Note that values that lie outside the map are valued at 0.

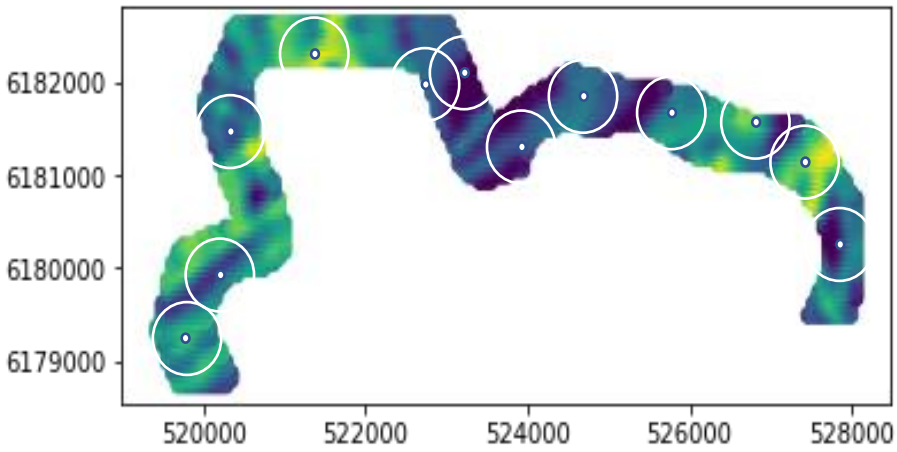

Figure 15 Search method given a ROV on a Kh map

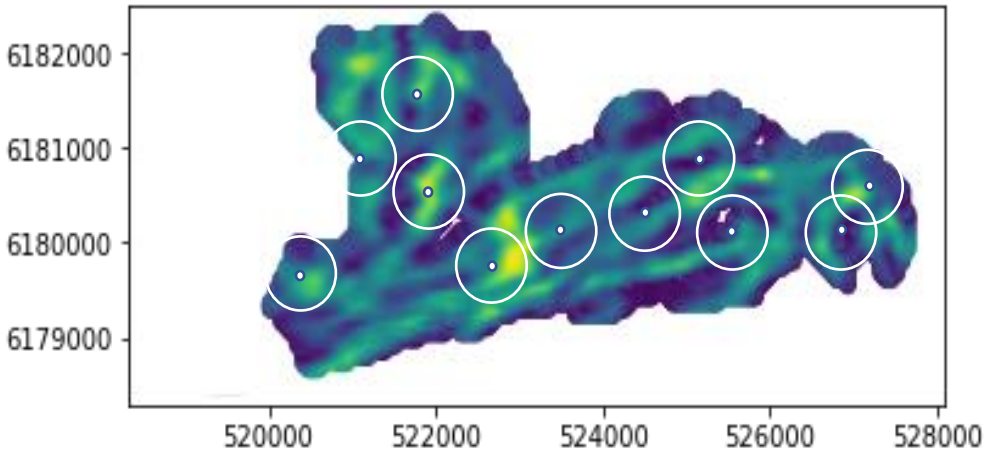

Figure 16 Search method given a ROV on a NHCT map

3.2.3. Input Parameters

The input parameters to the algorithm are the following:

- NHCT map
- Kh map
- Horizon map
- Maximum number of wells, N_W
- Maximum number of producers, N_P
- Horizontal well length, Hz_L
- Producer well spacing: After the placement of a producer well, the NHCT map is updated by eliminating a disk. The radius of the disk, R_D, around the well is defined by the producer well spacing (illustrated in Figure 17 and Figure 18).This disk is referred to as the black hole and prevents any other wells from being placed in the blacked-out region since it has a value of 0. Based on a given map, when using BHO, the well spacing controls the maximum number of wells that can be placed, however, a technical well spacing was introduced to BHPSO as an optimization parameter which eliminates this limitation [1]. The technical well spacing ensures the placement of any prescribed number of wells since this optimization parameter is calculated based on the number of wells involved.
- Injector well spacing: After every injector placement, the Kh map is updated by eliminating a cylinder. The radius of the cylinder is defined by the injector well spacing. A cylinder is used to form the black hole for the injectors instead of a

disk since the Kh map takes the form of a ring, as illustrated in Figure 17 and Figure 18.

- $\delta_{Azimuth}$: Increment to be used in optimizing the well azimuth.
- Radius Optimal Value (ROV)

3.2.3. Producer Placement in a Peripheral Water Injection Scheme

The algorithm starts by placing the producers in the following manner:

1. To create the producers' heels/toes:
    a. Find the **point** with the highest NHCT value, denoted as $Point_{opt}$, in the NHCT map.
    b. Place the producer at $Point_{opt}$. This point may represent the heel or the toe of the well. This could depend on, for example, the platform location in an offshore development planning problem.
2. Generate the horizontal well length and optimize its azimuth.
3. Place the horizontal well length in the right horizon.
4. Eliminate a disk of centre $Point_{opt}$ and radius equivalent to the input producer well spacing from the NHCT map. This is typically equivalent to setting a value = 0 for every point within this disk and is illustrated in Figure 17 and Figure 18.

Repeat until the number of input producers is reached. (Note that if the input producer well spacing does not allow for all the input number of producers to be placed

on the map, then the process will be repeated until the number of producers that fit on the given map is reached.)

3.2.4. Injector Placement in a Peripheral Water Injection Scheme

The Kh map is then used to place the injectors:

5. To create the injectors' heels/toes:
    a. Find the **region** with the highest Kh value, denoted as Region_{opt}, in the Kh map. (Radius of this region is given by an input ROV)
    b. Place the injector at the centre of $\text{Region}_{opt.}$
6. Repeat steps 2 and 3.
7. Eliminate a cylinder with a radius equivalent to the injector well spacing (Figure 17 and Figure 18).
8. Repeat until $N_W - N_P$ is reached. (Note that if the input injector well spacing does not allow for $N_W - N_P$ to be placed on the map, then the process will be repeated until the number of injectors that fit on the given map is reached.)

It was mentioned earlier that sufficient permeability is required for a peripheral injection scheme in order to allow the fluid being injected to move at an acceptable rate towards the producers. Hence, for the aforementioned reason, the option of placing injectors in **high permeability regions** instead of placing them based on high permeability points was adopted in this study. Moreover, a region search is later explored for the placement of producers. This is done by searching for high NHCT

regions to place the producers instead of placing them based on the highest NHCT point.

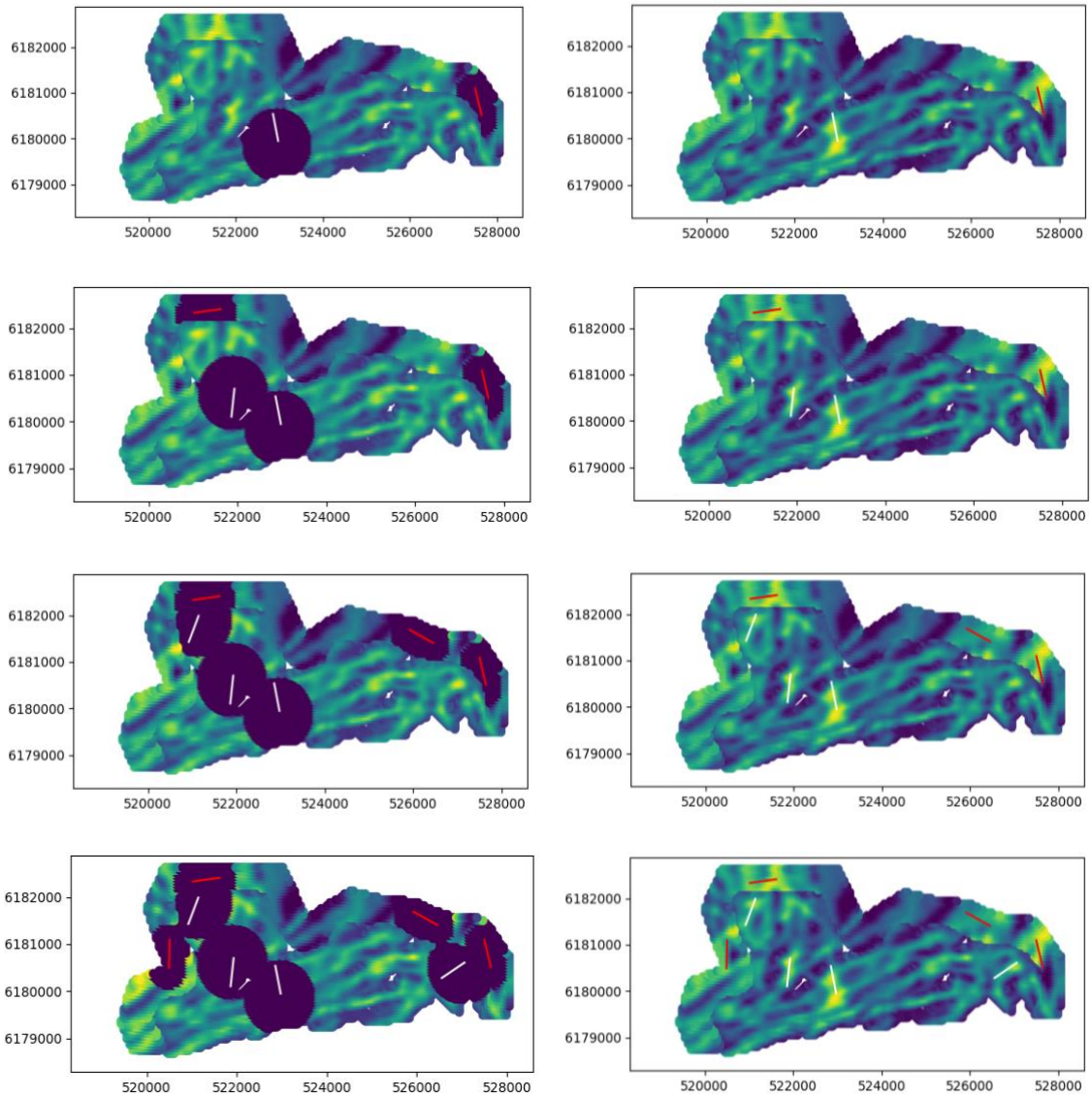

Figure 17 Process through which wells are being generated by the BHO given the input parameters – U22

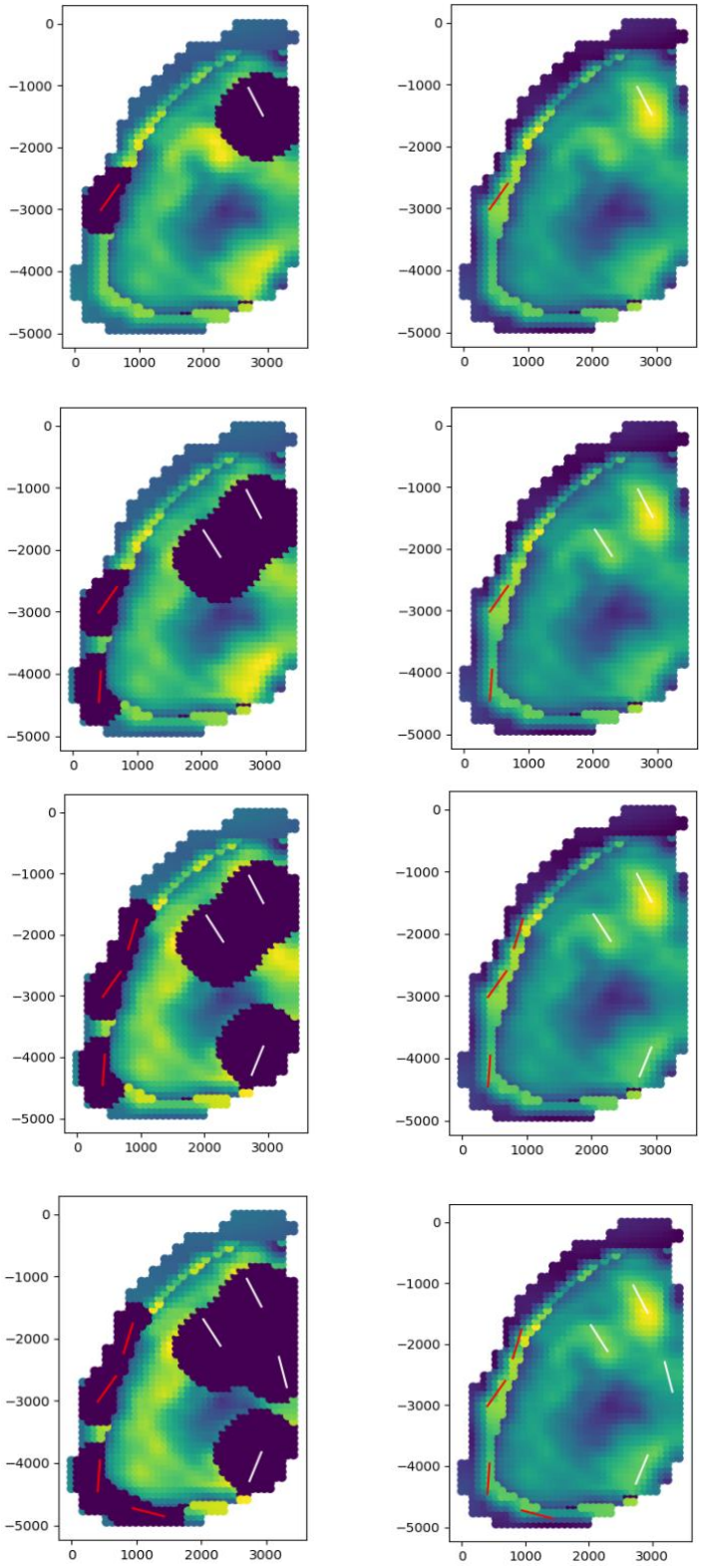

Figure 18 Process through which wells are being generated by the BHO given the input parameters – PUNQ-S3

3.3. BHPSO

The BHPSO process is summarized in Figure 19. The algorithms different building blocks are described below as applied to the placement of wells in a peripheral injection scheme.

3.3.1. Convergence Criteria

As mentioned earlier, the algorithmic parameter selection process for the algorithm highly affects the convergence criteria of PSO, however, setting convergence criteria for this algorithm is still a very challenging task which remains empirical to a large extent. Nevertheless, an attempt at enhancing the convergence criteria of BHPSO was addressed in chapter 4. Moreover, in this work, when one of the two conditions listed below is met, BHPSO declares convergence:

1. A prescribed number of iterations, $\text{Iteration}_{\max}$ is reached. In this work, $\text{Iteration}_{\max} = 100$ when testing on the PUNQ-S3 field, and $\text{Iteration}_{\max} = 50$ when testing on U22.
2. A lack of deviation between the particles, ε, is reached. In this work, $\varepsilon = 0.000001$.

It should be mentioned that the Olympus field was used only for verification testing with a number of maximum iterations half of that of the PUNQ-S3 field due to limitations in simulation time and computation power.

3.3.2. Initialization of the Optimization Parameters

The solution vector, of the BHO, is initialized by the PSO algorithm and includes the following parameters:

a. Row index of the i and j coordinates of the toe/heel of the first producer on the NHCT map
b. Row index of the i and j coordinates of the toe/heel of the first injector on the Kh map
c. Well count: a number bounded between a given minimum and maximum.
d. Horizontal section length: a number bounded between a given minimum and maximum.
e. Producer Horizon: a number bounded between the existing horizons of the field being used.
f. Injector Horizon: a number bounded between the existing horizons of the field being used.
g. Producer Well spacing factor (F_p): dimensionless parameter bounded by 0.5 and 2.5. This parameter is defined in section the section below.
h. Injector Well spacing factor (F_i): dimensionless parameter between 0.5 and 2.5. This parameter is defined in the section below.
i. Radius Optimal Value: a number bounded between a given minimum and maximum.

Note that in the original BHPSO, both producers and injectors were placed in the same horizon, however in real life scenarios wells are not necessarily placed in the same horizon, and for this reason, this enhancement was made in which the BHPSO workflow can optimize over the producer and injector horizon placement independently. Moreover, the parameters that are introduced to the BHPSO workflow through a peripheral injection scheme: b, h and i.

3.3.3. Placement of the First Well

The first producer (pattern injection), and the first producer and injector (peripheral injection) are the only wells whose placement is decided by PSO, and for this reason, the entire BHPSO workflow is independent of the number of wells. Note that the aforementioned characteristic of BHPSO drastically increases its efficiency. Moreover, the first producer's location (i- and j- coordinates) is selected by PSO, and then the BHO eliminates a disk around the selected i- and j- coordinates with a radius equivalent to the Producer Technical Well Spacing (PTWS) from the NHCT map. Similarly, the first injector's location (i- and j- coordinates) is selected by PSO. The BHO then eliminates a cylinder around the selected i- and j- coordinates with a radius equivalent to the Injector Technical Well Spacing (ITWS) from the Kh map.

Previously it was mentioned when using the BHO independently, the maximum number of wells that can be placed on a map is controlled by the well spacing, however, when using the BHPSO, a well spacing optimization parameter known as the 'well spacing factor' is introduced in order to calculate the TWS. The TWS ensures a place for all the wells on the map, via the well spacing factor, and was derived for BHPSO exclusively:

$$TWS = F\sqrt{\frac{A_r}{\pi N_w}} \tag{9}$$

$$PTWS = F_p\sqrt{\frac{A_r}{\pi N_p}} \tag{10}$$

$$TWS = F_i\sqrt{\frac{A_r}{\pi (N_w - N_p)}} \tag{11}$$

where A_r is the total NHCT cut off area, N_w the maximum number of wells, N_p the maximum number of producers, and F the well spacing factor. Equation 9 was originally derived for a pattern water injection scheme in which all the wells shared the same TWS since they are being placed on the same map. However, for a peripheral water injection scheme, where 2 maps exist, 2 separate technical well spacings will need to be calculated, hence the derivation of equation 10 and equation 11.

3.3.4. Placement of Remaining Wells

Once the first well/wells are placed, the remaining wells are placed by the BHO. The number of the remaining producers and injectors is decided by PSO, and they are sequentially placed using the NHCT map and KH map respectively. Also, the 'well spacing' value used in the BHO is replaced with the PTWS and ITWS for producers and injectors respectively, and so a 'black hole' around the producer of a radius equal to the PTWS is eliminated from the NHCT map and a cylinder around the injector of a radius equal to the ITWS is eliminated from the Kh map.

3.3.5. Case of Horizontal Wells – Well Azimuth Optimization, Horizons, and Well Length

In the case of horizontal wells, the horizontal trajectory (azimuth) is assessed by the BHO in which the NHCT correlating to the different azimuths is calculated. The azimuth is then placed in the trajectory of cells having the maximum cumulative NHCT. The azimuth increment, in this work, is a parameter that is set by the user and can be changed. Moreover, in this work an azimuth increment of 10° was selected. Horizons are specified vertical layers in which the horizontal section of the well is placed in.

Once the trajectory of the well is selected, the layer in which the well is placed in is optimized by PSO. The horizontal well length is another parameter that is decided by PSO.

3.3.6. PSO Updates

Each PSO iteration is composed of a series of particles known as simulation cases, in which, at each iteration, every single particle updates its optimization parameters. The update of the optimization parameters is followed by the update of the velocity and position of each particle. In the optimization process, once this happens, each particles' updated position defines the values of the parameters of the next iteration. This process is repeated until convergence is met.

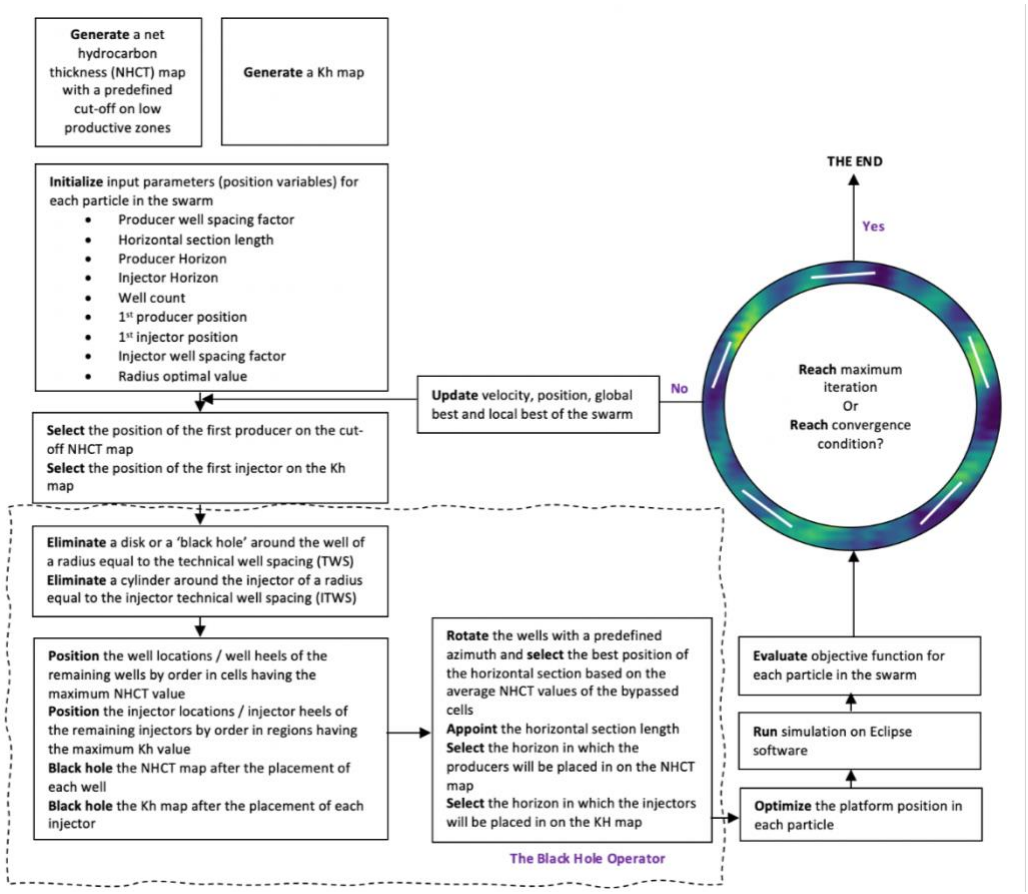

Figure 19 BHPSO workflow

CHAPTER 4

RESULTS AND DISCUSSION

In this chapter, the efficiency of the presented BHPSO methodology will first be tested accordingly through its application on both the Olympus and PUNQ-S3 fields for a peripheral water injection. Then, the Radius Optimal search option will be explored on a pattern water injection scheme, and on the producers in a peripheral injection scheme (since, as mentioned earlier, that the injectors in a peripheral injection scheme are placed on the Kh map using a Radius Optimal Option search method). Note that the main purpose of the 2nd activity is to test whether wells should be placed based on high property points, or based on a region search characteristic, which is the new concept we demonstrated throughout this thesis. In the final activity, the traditional Constant Inertia Weight (CIW) is replaced with a Linearly Increasing Inertia Weight (LDIW) in order to study its effect on PSO performance. This study is also associated with a sensitivity analysis on the acceleration coefficients, c_p and c_g.

The boundaries for the parameters that bound the search space of PSO are enlisted in Table 5, Table 6, Table 7, and Table 8, and are used throughout all the sections of this study.

Table 5 Pattern Water Injection PSO Initialization Boundaries – Olympus Upper

Well Count	10-16
Number of Producers	4-8
Producer Horizon	1-6
Injector Horizon	1-6
First Producer Index	x-y coordinates of the NHCT map
Technical Well Spacing Factor	1-2.5
Horizontal Well Length	400-700

Table 6 Pattern Water Injection PSO Initialization Boundaries – PUNQ-S3

Well Count	6-12
Number of Producers	4-8
Producer Horizon	1-5
Injector Horizon	1-5
First Producer Index	x-y coordinates of the NHCT map
Technical Well Spacing Factor	1-2.5
Horizontal Well Length	300-600

Table 7 Peripheral Water Injection PSO Initialization Boundaries – Olympus Upper

Well Count	12-16
Number of Producers	6-8
Producer Horizon	1-6
Injector Horizon	1-6
First Producer Index	x-y coordinates of the NHCT map
First Injector Index	x-y coordinates of the Kh map
Producer Well Spacing Factor	1-2.5
Injector Well Spacing Factor	1-2.5

Horizontal Well Length	400-700
Radius Optimal Value	100-400

Table 8 Peripheral Water Injection PSO Initialization Boundaries – PUNQ-S3

Well Count	8-14
Number of Producers	3-7
Producer Horizon	1-5
Injector Horizon	1-5
First Producer Index	x-y coordinates of the NHCT map
First Injector Index	x-y coordinates of the Kh map
Producer Well Spacing Factor	1-2.5
Injector Well Spacing Factor	1-2.5
Horizontal Well Length	300 - 600
Radius Optimal Value	50 - 200

4.1. Implementing a Peripheral Injection Scheme in the BHPSO Workflow

In order to test the functionality of the code, a swarm size of 5 particles was used for the simulation. A sensitivity analysis on the number of particles will be conducted at a later stage. The boundaries shown in Table 5, Table 6, Table 7, and Table 8 were used and the optimization run for each field was repeated 3 times over a fixed number of 20 iterations due to the stochastic nature of BHPSO.

4.1.1. Olympus U22

The peripheral injection BHPSO runs on U22 returned 3 different well placements which can be seen in Figure 20, Figure 21, and Figure 22. Also, in the figures below, each case is accompanied by its corresponding BHPSO performance.

Note that the green, yellow, and red points on the graph represent the best, middle, and worst combination of decision variables obtained in an iteration, respectively.

For case 1, the final and best iteration in the optimization run returned a total well count of 15 with a well length of 700 m and a ROV of 258 m. Moreover, the producers and injectors are placed in horizon 2 and 4 respectively with an optimum producer well spacing of 1208 m and optimum injector well spacing of 498 m. Case 1 yielded a NPV of $1090 MM with well costs equivalent to $363.072 MM, respectively.

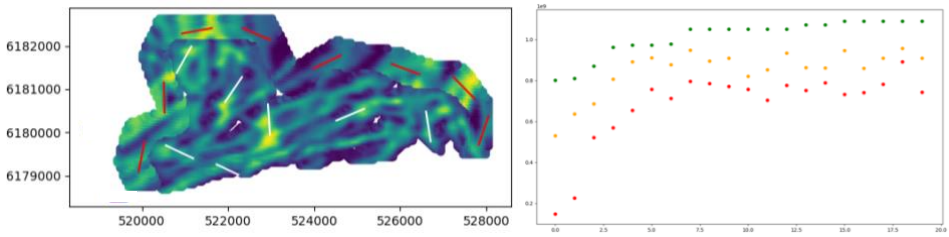

Figure 20 Case 1 of a BHPSO Peripheral Injection – U22

For case 2, the global optimum reached in a series of 20 iterations resulted in a NPV of $1049.30 MM. Well costs reached $367.12 MM with 16 wells being placed in the field. The producers and injectors are placed in horizon 3 and 4 respectively, have a well length of 532 m, a ROV of 371 m, and a producer and injector well spacing of 1261 m and 498 m respectively.

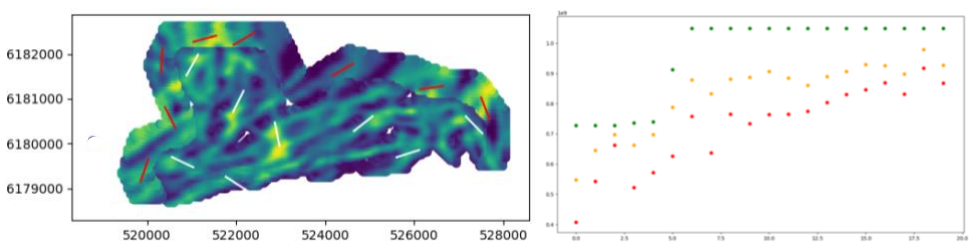

Figure 21 Case 2 of a BHPSO Peripheral Injection – U22

Case 3 returned an optimal well count of 12, a producer well spacing of 1328 m, an injector well spacing of 629 m, a ROV of 334 m and horizontal well lengths of 453 m that are placed in horizon 5 and horizon 3 for the producers and injectors respectively. The NPV obtained in this scenario is valued at $995.7 MM with well costs of $269.39 MM.

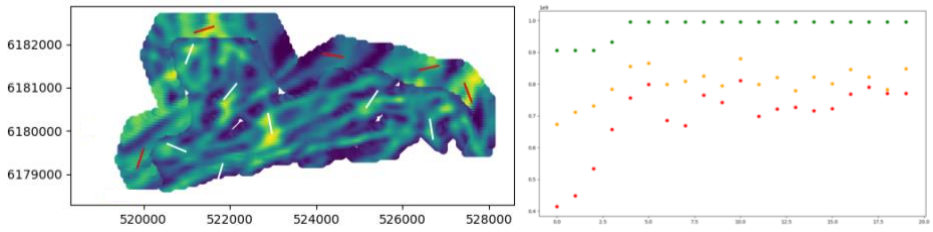

Figure 22 Case 3 of a BHPSO Peripheral Injection – U22

4.1.2. PUNQ-S3

Similarly, the peripheral injection well placement using BHPSO, for 3 runs, on the PUNQ-S3 field can be seen in Figure 23, Figure 24, and Figure 25 with each cases' relative BHPSO performance. For case 1, a 20-iteration run led to global optimum NPV of $1496.67 MM, and well costs of $144.88 MM. Moreover, producer well spacing, injector well spacing, ROV and horizontal well length are 1128 m, 255 m, 154 m, and 304 m, respectively. The 5 producers are placed in horizon 3, while the 6 injectors are placed in horizon 2.

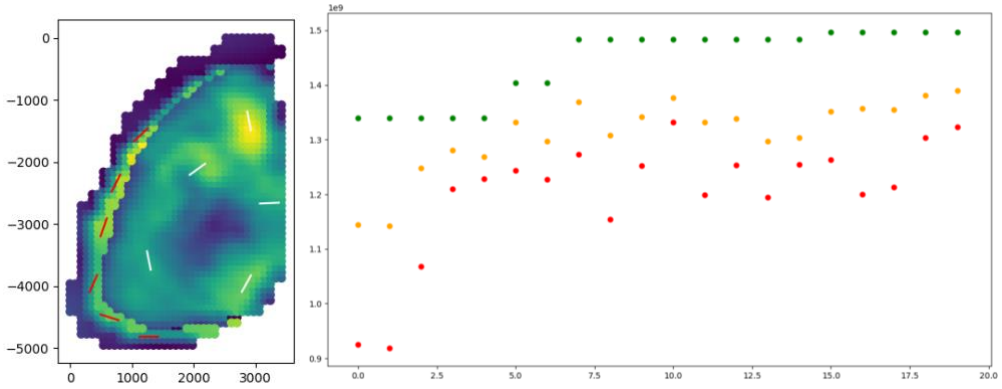

Figure 23 Case 1 of a BHPSO Peripheral Injection – PUNQ-S3

As for case 2, 8 wells are spread across both the KH and NHCT maps with the producers having a well spacing of 1350 m and injectors a well spacing of 361 m. The producers are placed in horizon 4 while the injectors are placed in horizon 5. The ROV is 169 m and the horizontal well length is 493 m. This case resulted in a NPV of $1445.27 MM, with corresponding well costs of $116.18 MM.

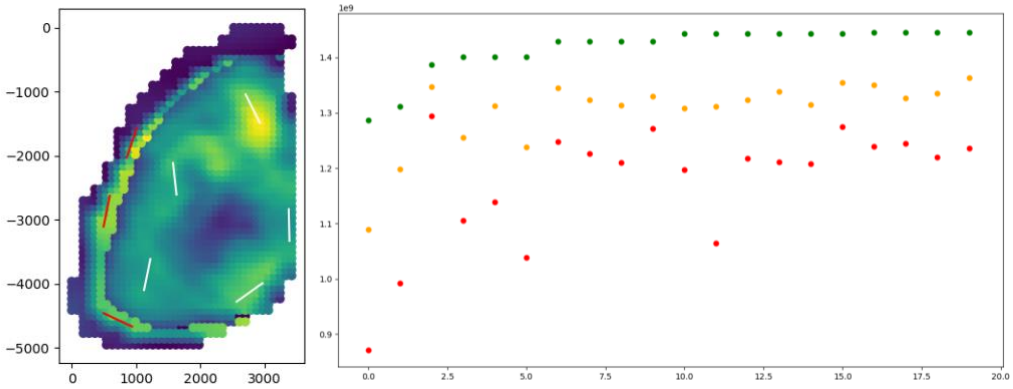

Figure 24 Case 2 of a BHPSO Peripheral Injection – PUNQ-S3

Case 3 returned a NPV of $1552.70 MM, and well costs of $179.33 MM. Producer and injector well spacings are 758 m and 511 m, respectively. The 7 generated producers are placed in horizon 4 and the 6 generated injectors are placed in horizon 3, and have a horizontal section length of 540 m. The ROV obtained is 192 m.

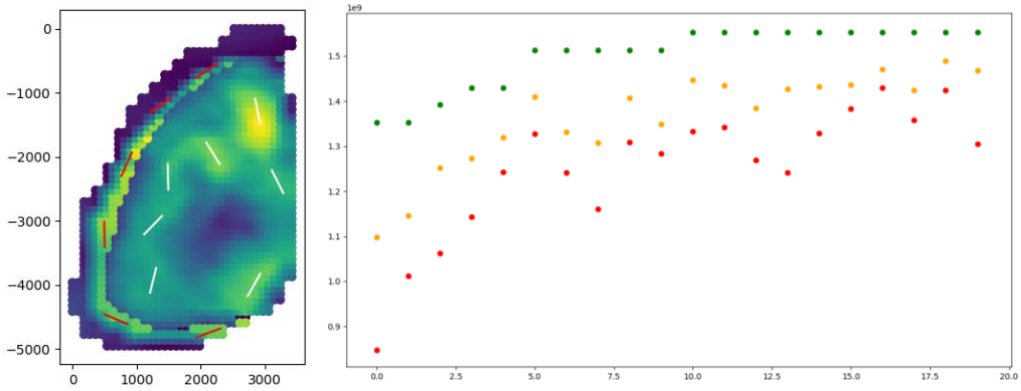

Figure 25 Case 3 of a BHPSO Peripheral Injection – PUNQ-S3

4.2. Testing and Evaluating Different Black Holing Techniques: Point vs Region Search

In order to demonstrate the difference between placing a well based on a high property point (point search) and based on a high property region (region search), a fixed set of input parameters were fed to the Black Hole Operator (independent of PSO), and tested on both well placement techniques in order to highlight the difference between them. This was done for both the Olympus and PUNQ-S3 field.

4.2.1. Pattern Water Injection

In Figure 26 and Figure 27, both simulation runs have a well spacing of 800 m, producer horizon = 1, injector horizon = 2, number of producers = 5, number of injectors = 5, and horizontal well length = 600 m, however, Figure 27 is given a radius optimal value of 400 m which allows for the change in the placement of wells. Figure 26, which is the case in which the wells are placed based on high NHCT points returned a NPV of $913 MM while Figure 27, which is the case in which the wells are placed based on high NHCT regions returned a NPV of $727 MM.

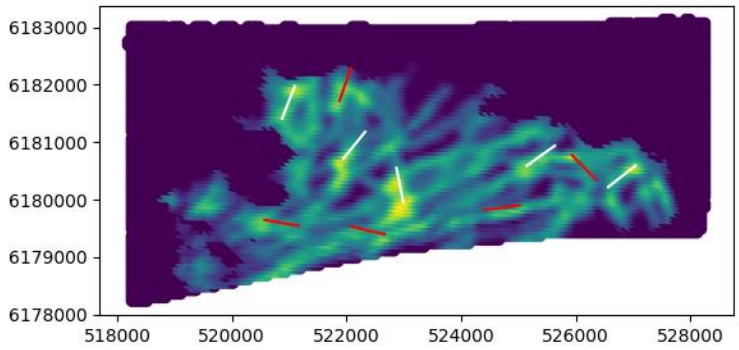

Figure 26 Point Search Method in a Pattern Injection Scheme – U22

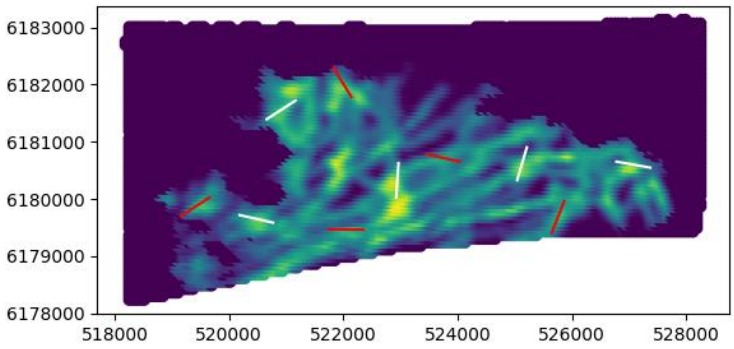

Figure 27 Region Search Method in a Pattern Injection Scheme – U22

In Figure 28 and Figure 29, a well spacing of 1300 m is applied to both the simulation runs along with a producer horizon = 1, injector horizon = 2, number of producers = 4, number of injectors = 4, and horizontal well length = 500 m. Moreover, Figure 29 is given a radius optimal value of 150 m. Figure 28, which is the case in which the wells are placed based on high NHCT points returned a NPV of $1427 MM while Figure 29, which is the case in which the wells are placed based on high NHCT regions returned a NPV of $1472 MM.

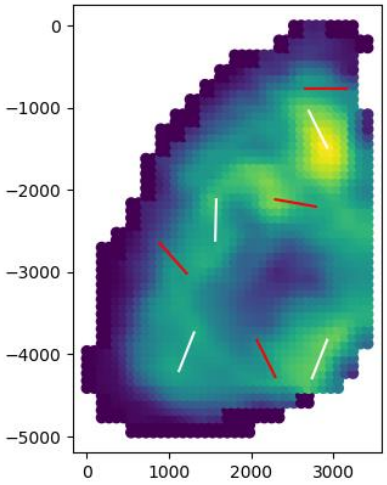

Figure 28 Point Search Method in a Pattern Injection Scheme – PUNQ-S3

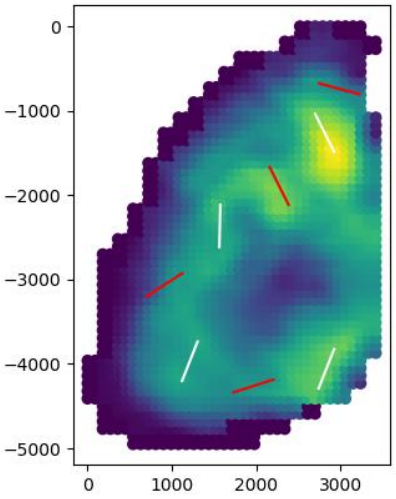

Figure 29 Region Search Method in a Pattern Injection Scheme – PUNQ-S3

4.2.2. Peripheral Water Injection

For a peripheral water injection scheme, 3 different search method combinations will be studied:

1- The first is the combination that is originally adopted in this work which is placing the producers based on the highest NHCT point on the NHCT map, and placing the injectors based on the highest Kh regions on the Kh map. However,

whether it is a reliable strategy or not to place the injectors based on high permeability regions, it is not confirmed, and for this reason:

2- the second combination of search methods will be placing both the producers and injectors using a point search method, while

3- the third combination is placing both the producers and injectors using a region search method.

The three combinations which can be seen in the figures below display a producer well spacing of 800 m, an injector well spacing of 400 m, producer and injector horizons of 1 and 2 respectively, and a horizontal well length of 600 m with 5 producers and 5 injectors. Figure 30, being the first combination and having an injector ROV of 400 m, returned a NPV of $817 MM, while Figure 31, being the second combination yielded an NPV of $775 MM. Moreover, Figure 32, the third combination, having a producer ROV = 300 m and Injector ROV= 400 m, returned a NPV of $949 MM. It should be noted that combination 1 and 2 will have the producers placed in the same manner, while combination 1 and 3 will have the injectors placed in the same manner.

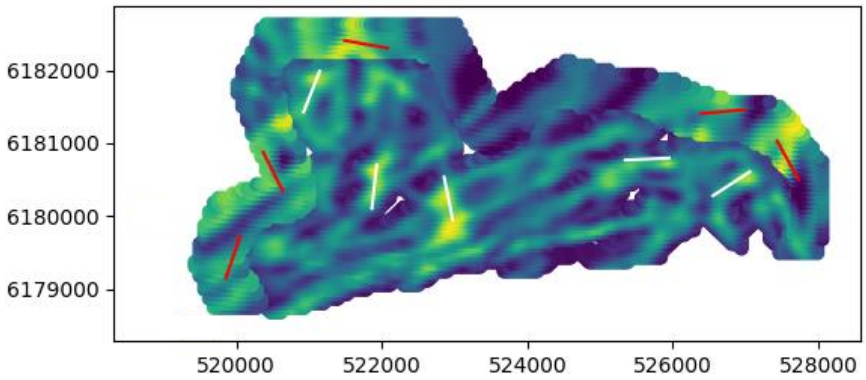

Figure 30 Point Search Method (Producers) and Region Search Method (Injectors) in a Peripheral Injection Scheme – U22

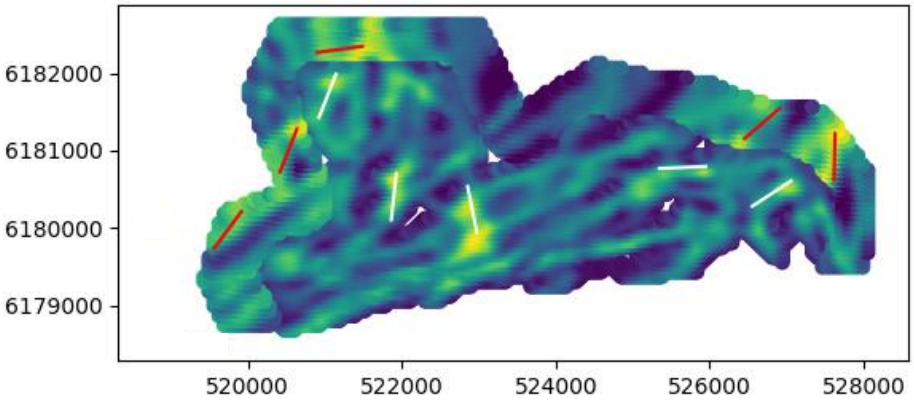

Figure 31 Point Search Method in a Peripheral Water Injection Scheme – U22

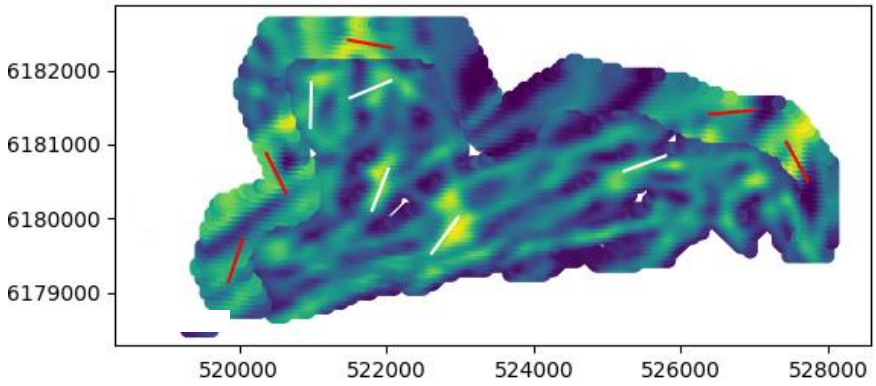

Figure 32 Region Search Method in a Peripheral Water Injection Scheme – U22

Similarily, for the PUNQ-S3 field, the three combinations which can be seen in the figures below displayed a producer well spacing of 1300 m, an injector well spacing of 650 m, producer and injector horizons of 1 and 2 respectively, and a horizontal well length of 500 m with 4 producers and 4 injectors. Figure 33, being the first combination and having an injector radius optimal value of 200 m, returned a NPV of $1352 MM, while Figure 34, being the second combination yielded an NPV of $1340 MM. Moreover, Figure 35, the third combination, having a producer Radius Optimal Value = 200 m and Injector Radius Optimal Value = 200 m, returned a NPV of $1373 MM.

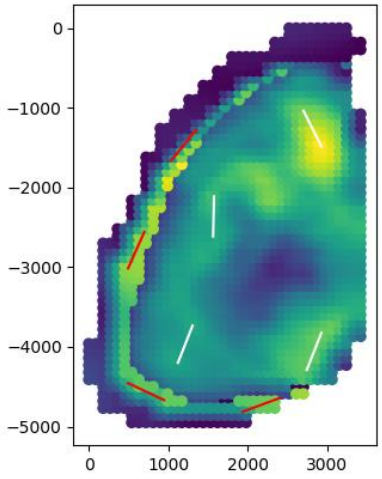

Figure 33 Point Search Method (Producers) and Region Search Method (Injectors) in a Peripheral Injection Scheme – PUNQ-S3

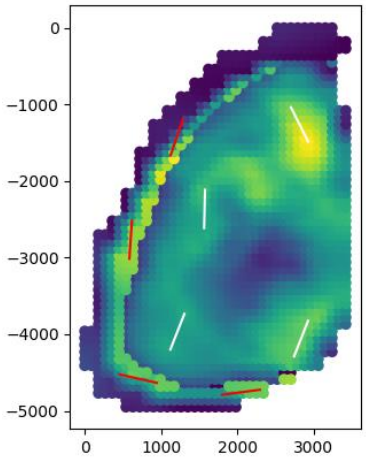

Figure 34 Point Search Method in a Peripheral Water Injection Scheme – PUNQ-S3

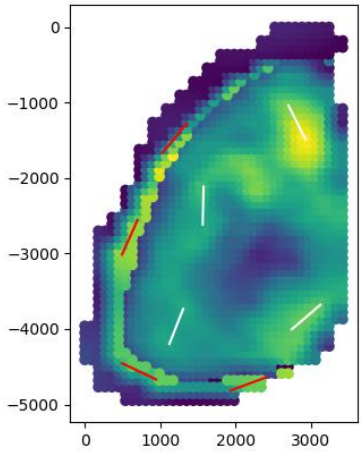

Figure 35 Region Search Method in a Peripheral Water Injection Scheme – PUNQ-S3

It can be seen that in some cases a point search method yields higher NPV than that of the region search method, and vice versa. However, it should be noted that the input parameters are not optimized over and the above study was done soley to highlight the affect of the search methods on the well placements given fixed parameters. Furthermore, in order to study the effect that the search methods have on the NPV and which method should be adopted for the BHPSO algorithm, a study was carried out using BHPSO on the different combinations listed above. However, before carrying out this study, a sensitivity analysis was conducted on the number of particles to be used.

4.2.3. Sensitivity Analysis – Number of Particles

In this work, 5,10,15 and 20 particles are simulated to test for NPV redundancy. It should be noted that the particle sensitivity analysis is conducted according to the the original BHPSO methodology, and was done for both pattern and peripheral water injection schemes. Moreover, extensive testing is done using the PUNQ-S3 field while U22 is used for verification purposes only due to its limitations in simulation time.

Each swarm size was simulated 10 times across 100 iterations as can be seen in the figures below. Figure 36, Figure 37, Figure 38, and Figure 39 display results for 5,10,15 and 20 particles, respectively, for a pattern water injection scheme. The average NPV for a a swarm size of 5 particles returned an average NPV of $1511 MM, while swarm sizes of 10, 15 and 20 particles returned NPV's of $1583 MM, $1622 MM, and $1616 MM, respectively. For a peripheral water injection scheme,

Figure 40, Figure 41, Figure 42, and Figure 43 display results for 5,10,15 and 20 particles, respectively. The average NPV's attained are $1564 MM, $1619 MM, $1623

MM, and $1648 MM for 5, 10, 15, and 20 particles respectively. It can be noticed that an increase in swarm size led to an increase in the average NPV across both injection schemes, furthermore, the NPV results varied significantly for any swarm size below 20 particles. A swarm size of 20 particles returned redundant results in both injection schemes, and for this reason, all simulated results in this study will be carried out using a swarm size of 20 particles.

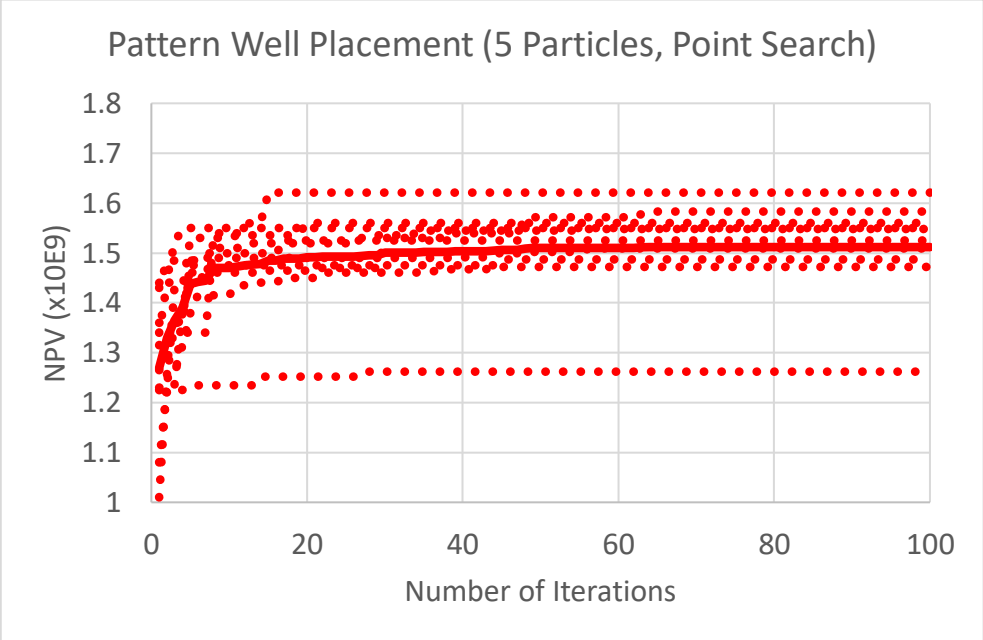

Figure 36 Pattern Water Injection Particle Sensitivity Analysis – 5 Particles

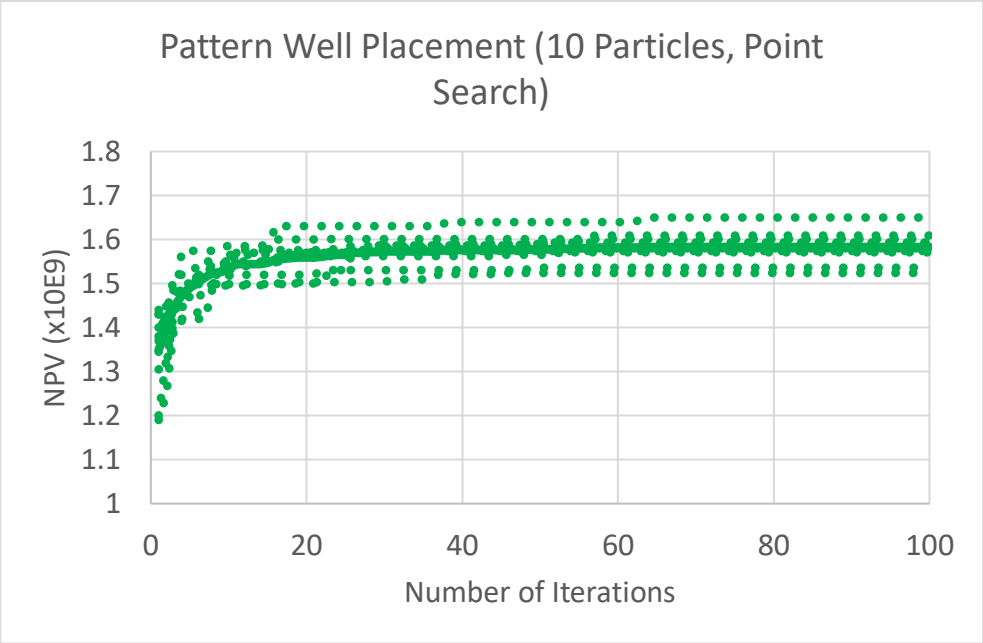

Figure 37 Pattern Water Injection Particle Sensitivity Analysis – 10 Particles

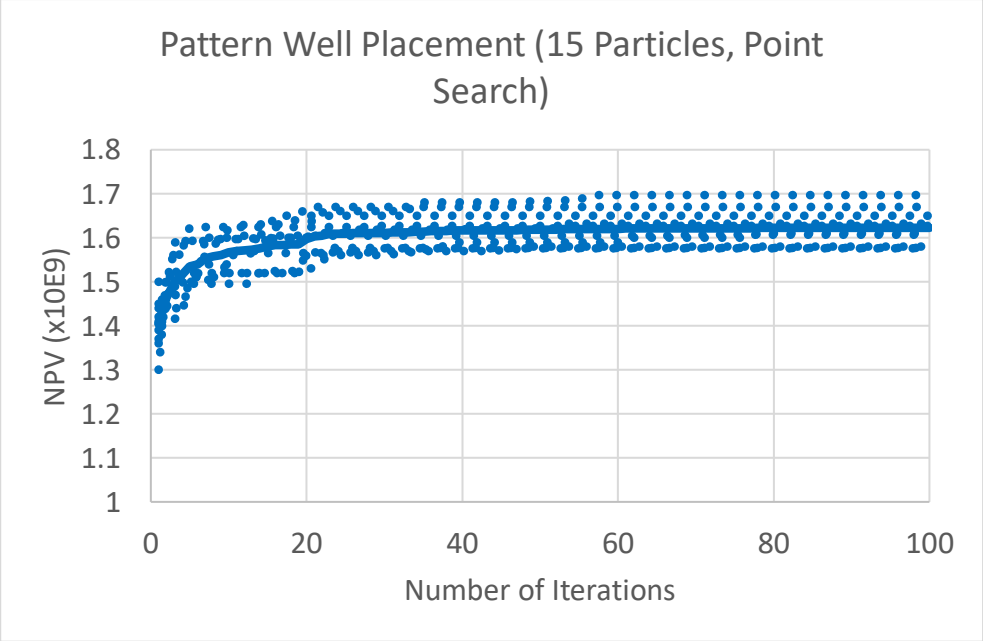

Figure 38 Pattern Water Injection Particle Sensitivity Analysis – 15 Particles

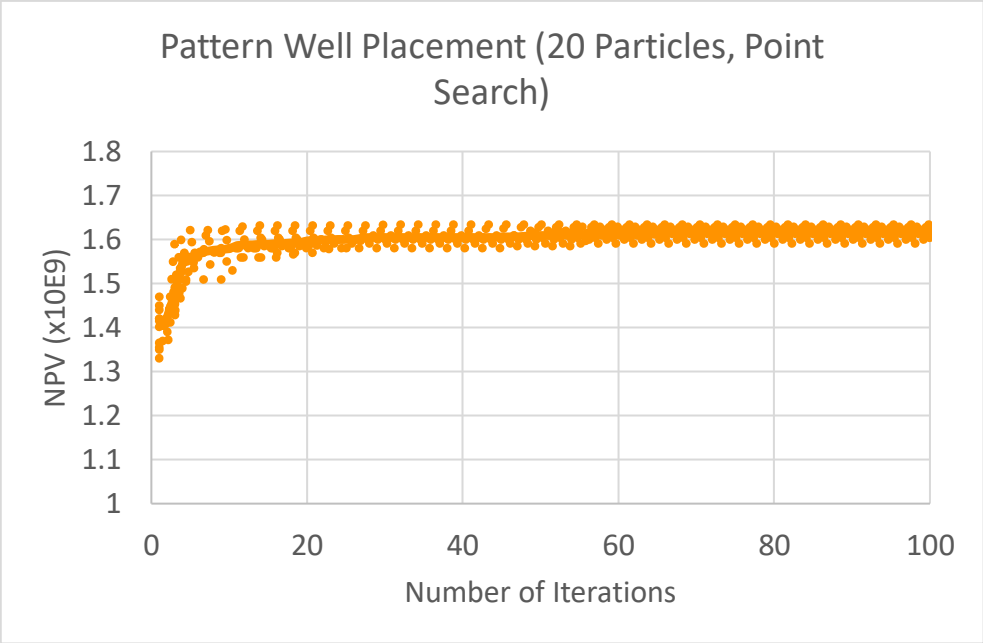

Figure 39 Pattern Water Injection Particle Sensitivity Analysis – 20 Particles

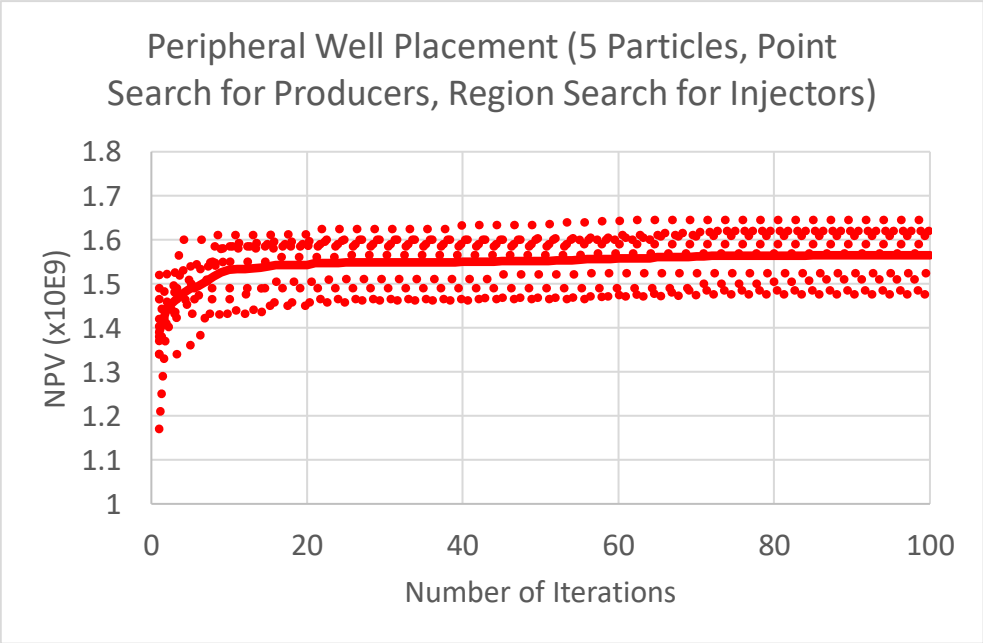

Figure 40 Peripheral Water Injection Particle Sensitivity Analysis – 5 Particles

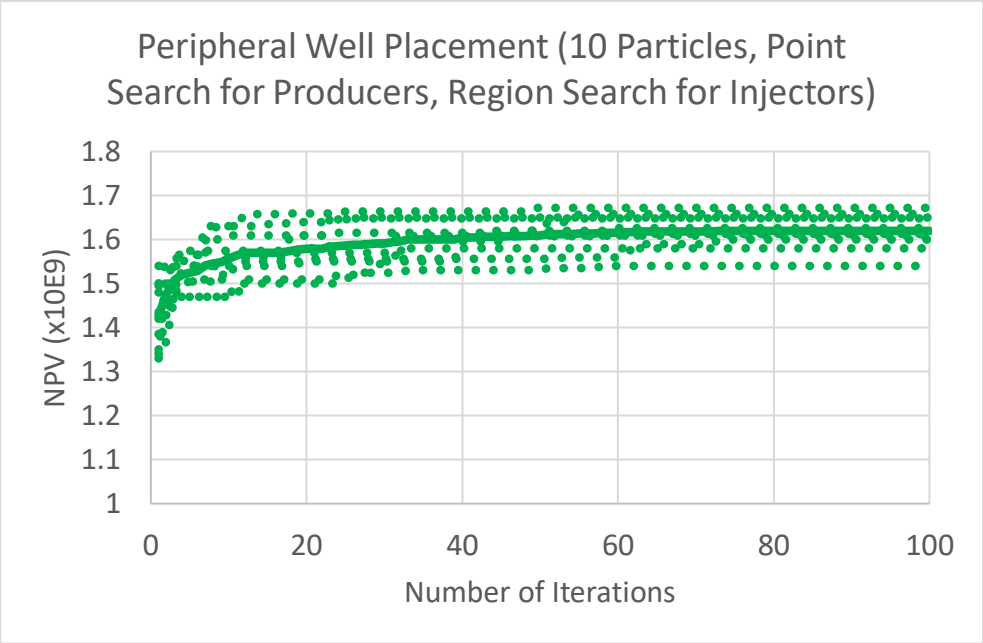

Figure 41 Peripheral Water Injection Particle Sensitivity Analysis – 10 Particles

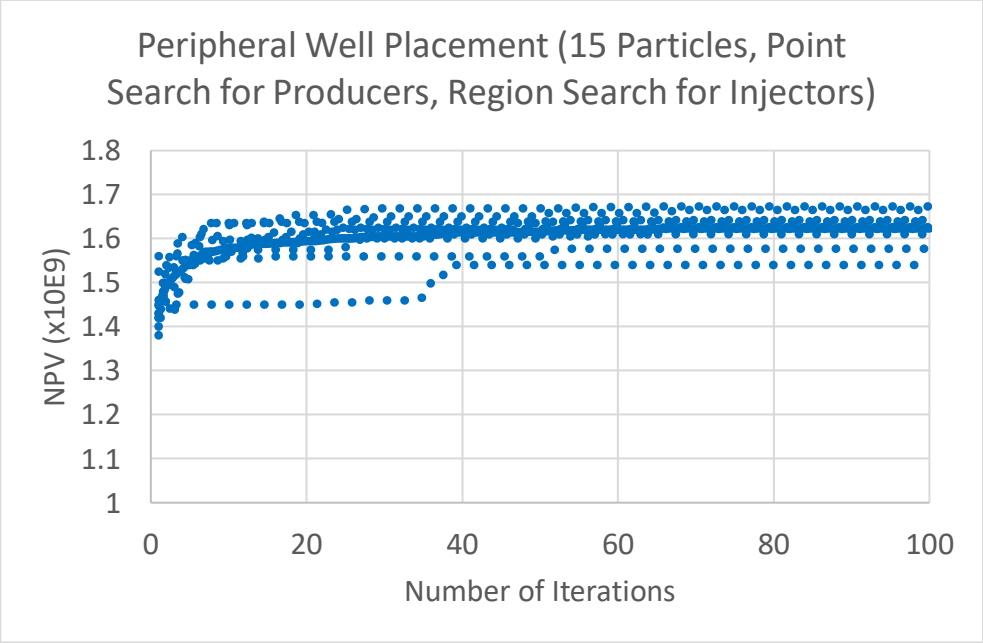

Figure 42 Peripheral Water Injection Particle Sensitivity Analysis – 15 Particles

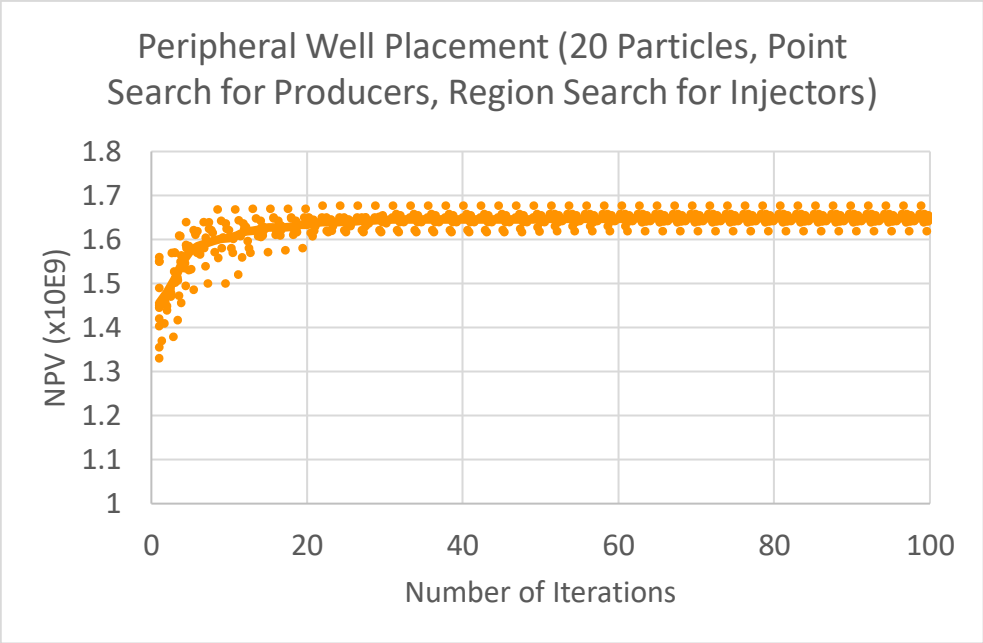

Figure 43 Peripheral Water Injection Particle Sensitivity Analysis – 20 Particles

4.2.4. BHPSO Application for Search Method Testing

As mentioned in the section above, BHPSO must be applied to the search methods, independently, in order to compare between them. Using 20 particles, BHPSO was applied to the PUNQ-S3 field simulating 10 times across 100 iterations for a pattern and peripheral injection scheme using the search methods and combinations discussed above. The results obtained are displayed in Figure 44 through **Error! Reference source not found.**.

It can be seen, for a pattern water injection, that the results obtained for both search methods are in close proximity. For a point search method, an average NPV of $1616 MM was obtained, while for a region search method, an average NPV of $1635 MM was obtained. A 1% increase in the average NPV was found when using a region search method.

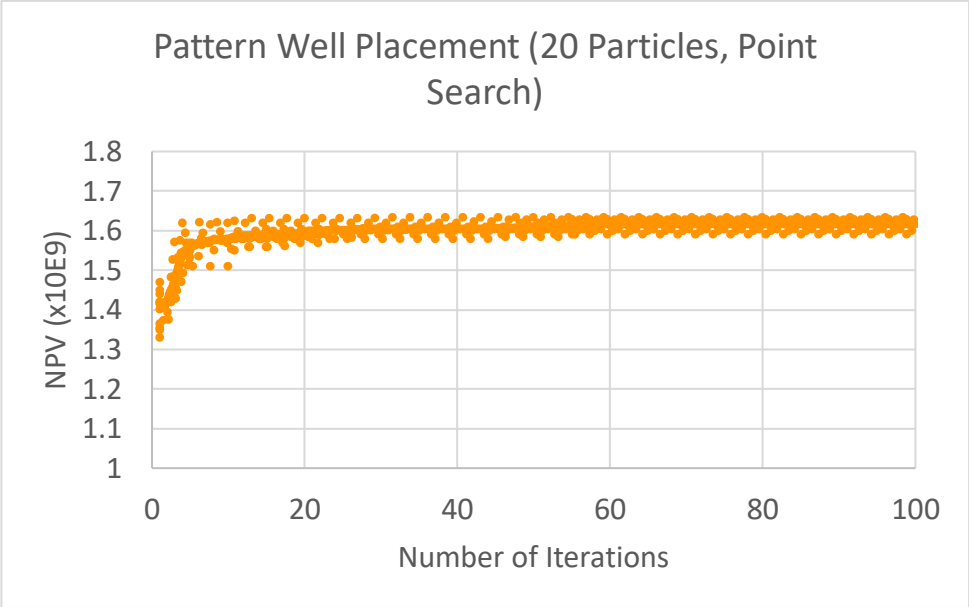

Figure 44 BHPSO Pattern Water Injection Results – Point Search Method (PUNQ-S3)

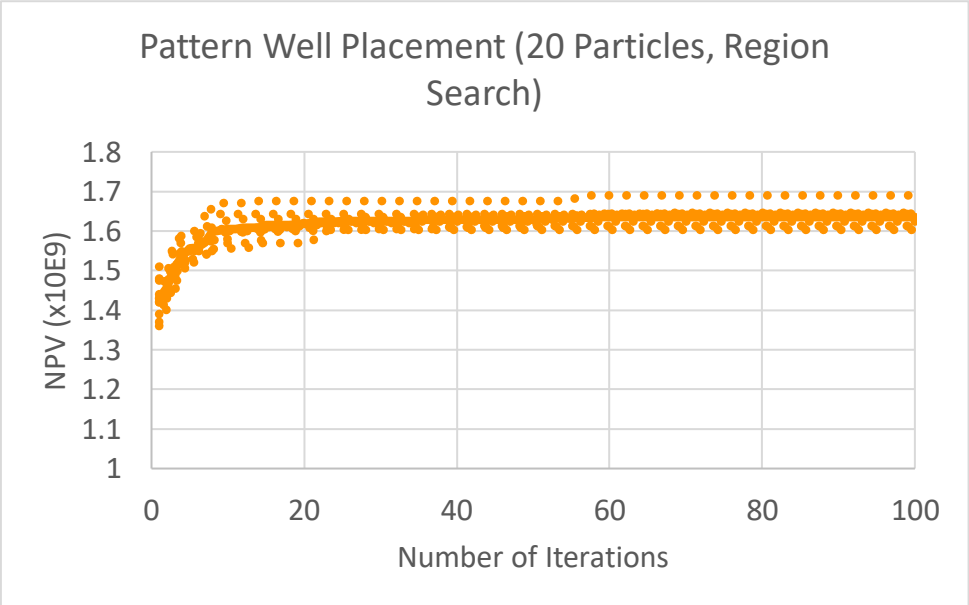

Figure 45 BHPSO Pattern Water Injection Results – Region Search Method (PUNQ-S3)

For a peripheral water injection scheme, it can be seen, as predicted, that the placement of injectors based on high permeability regions is essential, and that

combination 2 (Point search for both producers and injectors; Figure 47) can be discarded. However, for combination 1 (Figure 46) and combination 3 (**Error! Reference source not found.**) which differ in the placement technique of the producers, an average NPV of $1648 MM was obtained for combination 1, while an average NPV of $1645 MM was obtained for combination 3, hence a bare difference of 0.18% in the average NPV between combination 1 and combination 3.

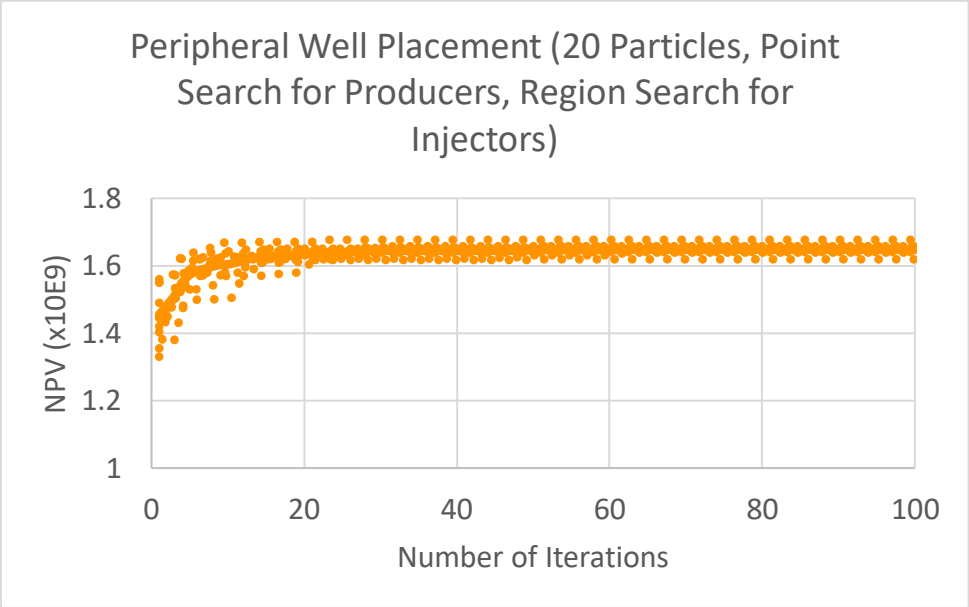

Figure 46 BHPSO Peripheral Water Injection Results – Point Search Method (Producers) and Region Search Method (Injectors) (Combination 1-PUNQ-S3)

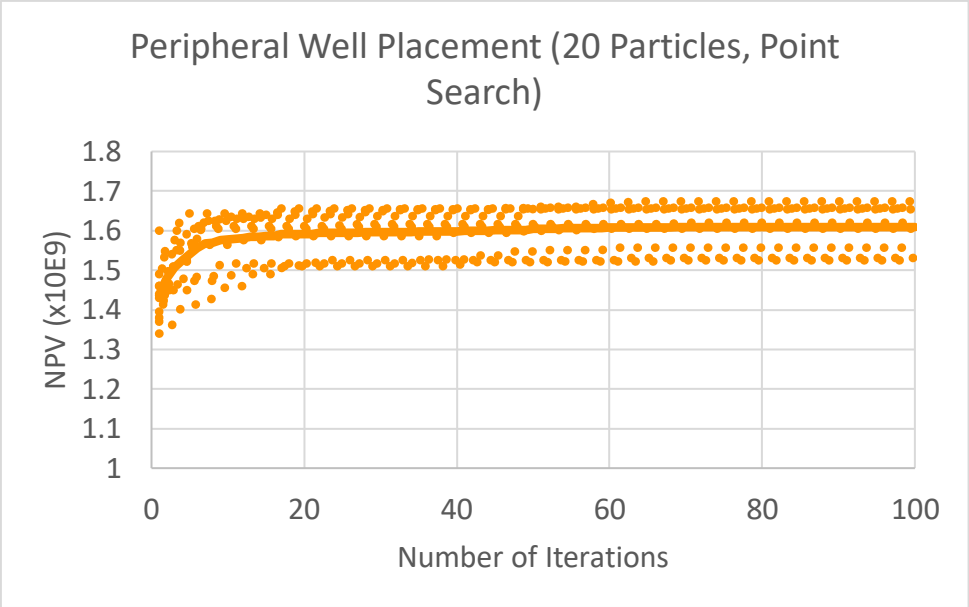

Figure 47 BHPSO Peripheral Water Injection Results – Point Search Method (Combination 2-PUNQ-S3)

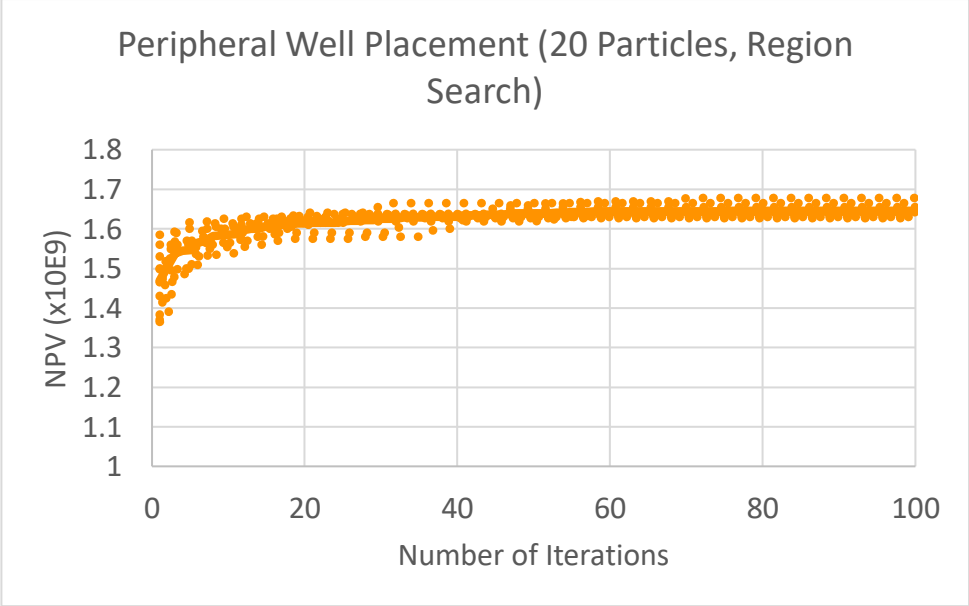

Figure 48 BHPSO Peripheral Water Injection Results – Region Search Method (Combination 3-PUNQ-S3)

It should be noted when using a region search method, for a pattern water injection scheme, an extra decision variable is added to the system hence increasing the systems complexity and simulation time, whereas for a peripheral water injection scheme, 1 decision variable is added to the system for combination 1, while 2 decision variables are added to the system when using combination 2. So, it can be concluded that for a pattern water injection, the original search method of placing the wells based on high NHCT points will not be altered, while for a peripheral water injection scheme, the injectors will be placed based on high permeability regions, while the producers will be placed based on high NHCT points (combination 1). Moreover, this conclusion was made based on the fact that adding complexity to the system for a mere increase in the average NPV has no significance.

Nevertheless, in order to justify the interpretation made above, the search method techniques were tested on U22 for a pattern water injection scheme. For reasons mentioned in section 3.3.1., BHPSO was simulated 3 times across 50 iterations. The results obtained verfiy the observation made above. The point search technique returned an average NPV of $1103 MM and the region search technique returned an average NPV of $1167 MM, resulting in an insignificant 5.5% increase in the average NPV for a region search method.

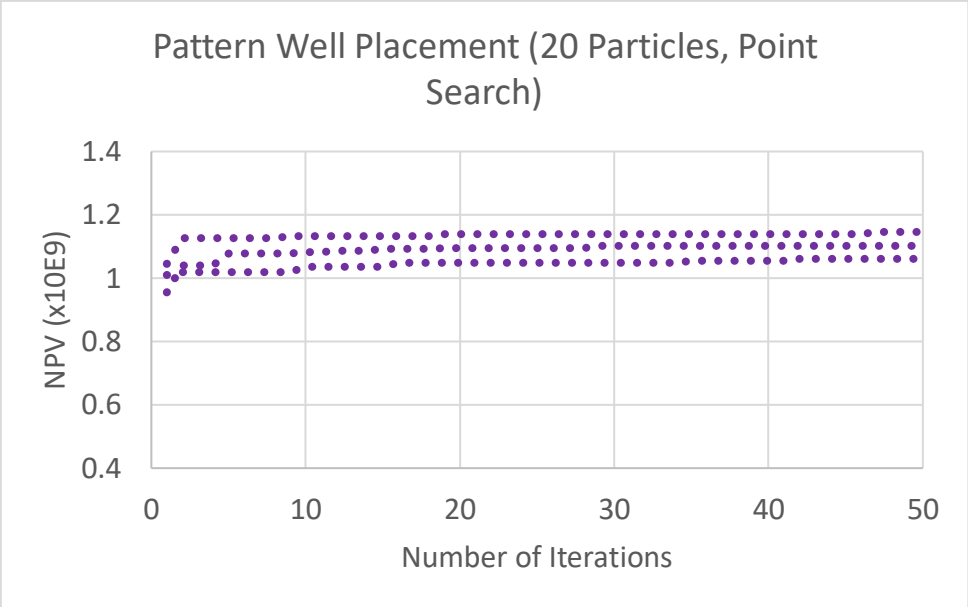

Figure 49 BHPSO Pattern Water Injection Results – Point Search Method U22

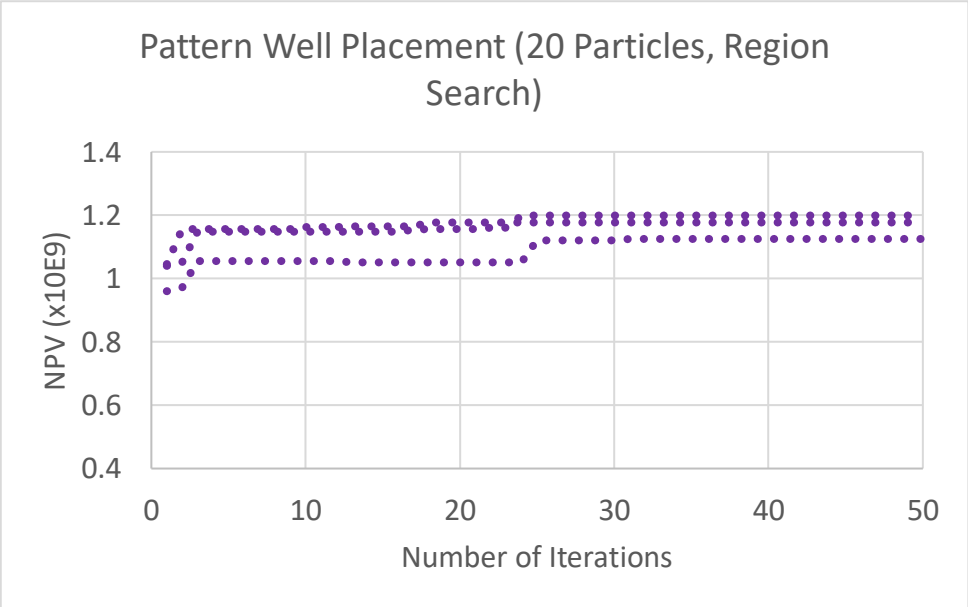

Figure 50 BHPSO Pattern Water Injection Results – Region Search Method U22

4.3. Defining a Convergence Criterion for the BHPSO Workflow

In the final part of this work, a linearly decreasing inertia weight was introduced to the BHPSO in order to enhance the convergence of the particles. Testing was carried out on the PUNQ-S3 field only since this inertia weight strategy is being applied in order to study its characteristics only.

4.3.1. Sensitivity Analysis on Acceleration Coefficients

A sensitivity analysis on the acceleration coefficients was first conducted in order to find a good combination between these coefficients and the inertia weight strategy. This was done because the combination of these algorithmic parameters has a significant influence on the algorithm. Acceleration coefficients of $c_p = c_g = 0.5$, 0.775, 1, 2, 2.5, and 3 were tested independently across 30 iterations. The results obtained are displayed in the figures below. It can be seen that for $c_p = c_g = 0.5$, 0.775, 1, 2.5, and 3 (Figure 51, Figure 52, Figure 53, Figure 55, and Figure 56), the NPV results were not redundant, however, for a $c_p = c_g = 2$ (Figure 54), they were. Acceleration coefficients with values of 0.5, 0.775, 1, 2.5 and 3 were discarded, and the study was carried on by setting the acceleration coefficients to 2.

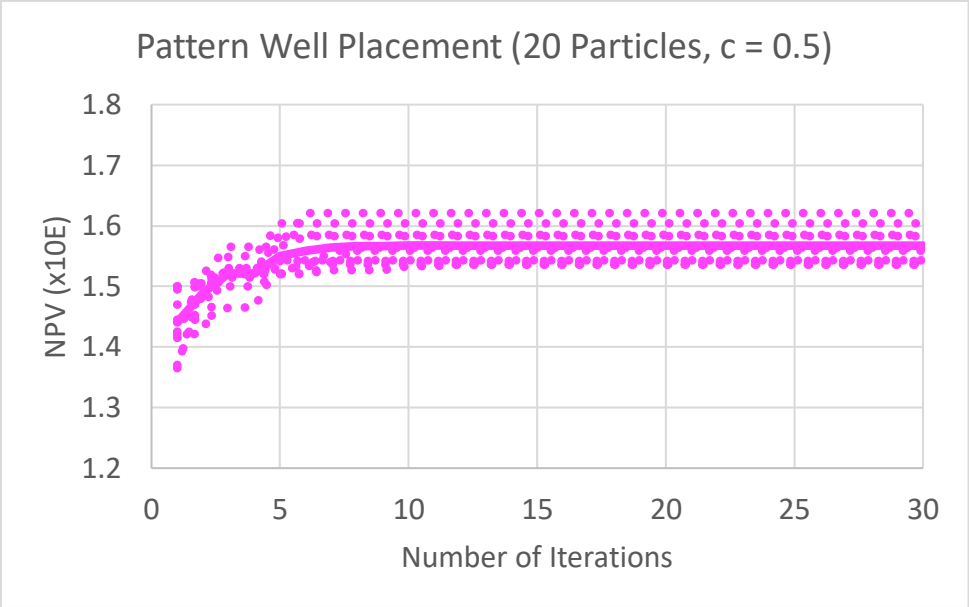

Figure 51 BHPSO Pattern Water Injection Results with c = 0.5 – LDIW

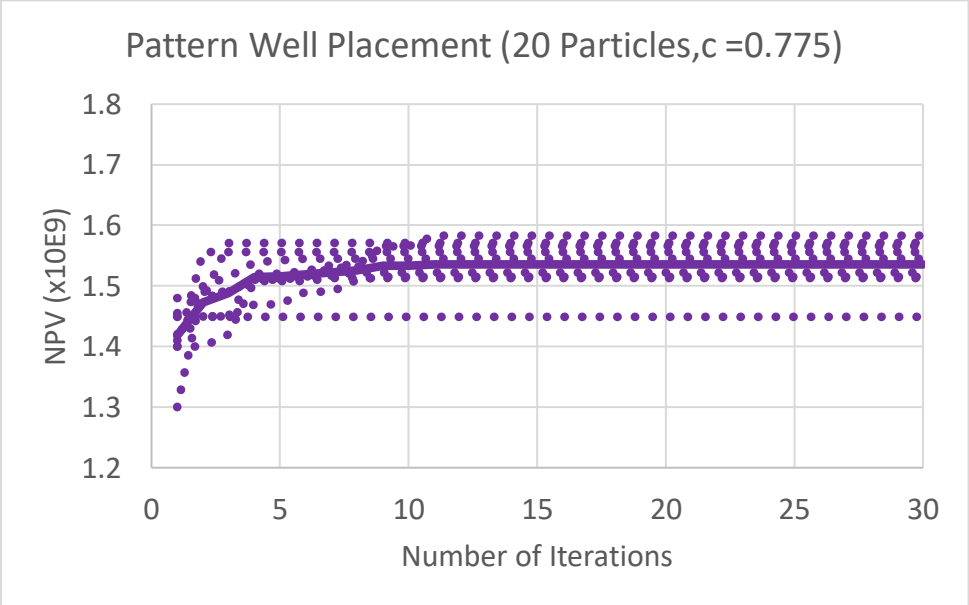

Figure 52 BHPSO Pattern Water Injection Results with c = 0.775 – LDIW

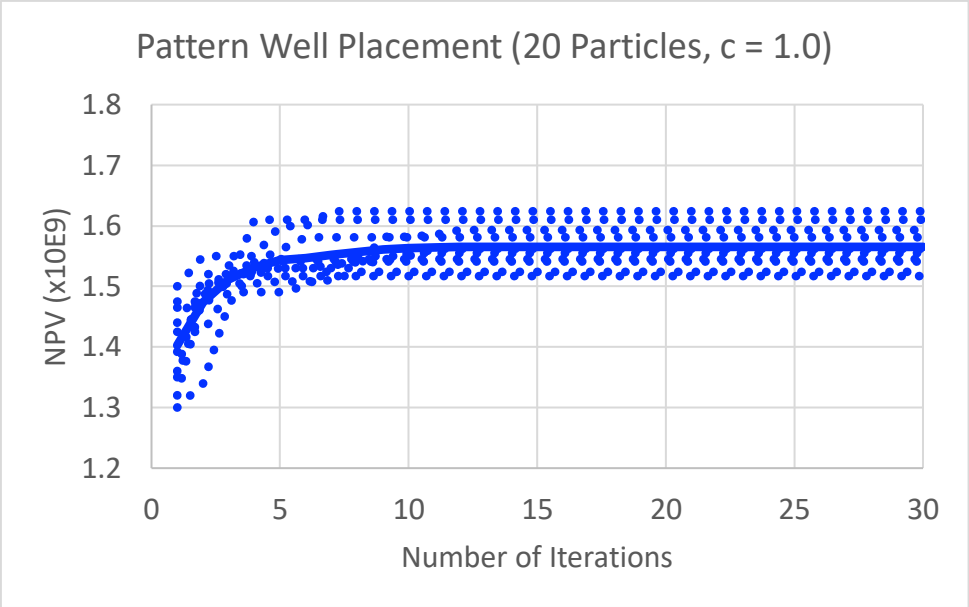

Figure 53 BHPSO Pattern Water Injection Results with c = 1 – LDIW

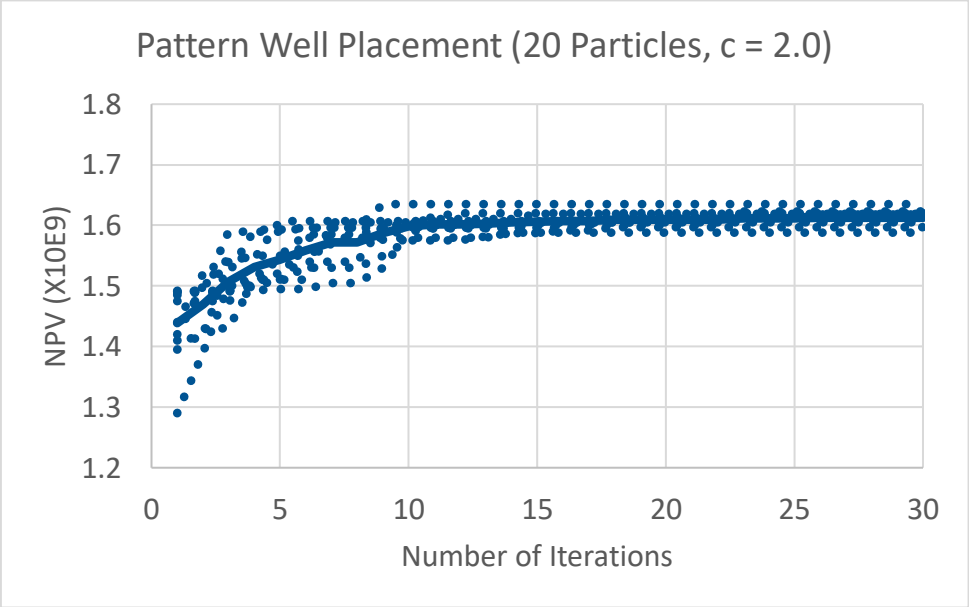

Figure 54 BHPSO Pattern Water Injection Results with c = 2 – LDIW

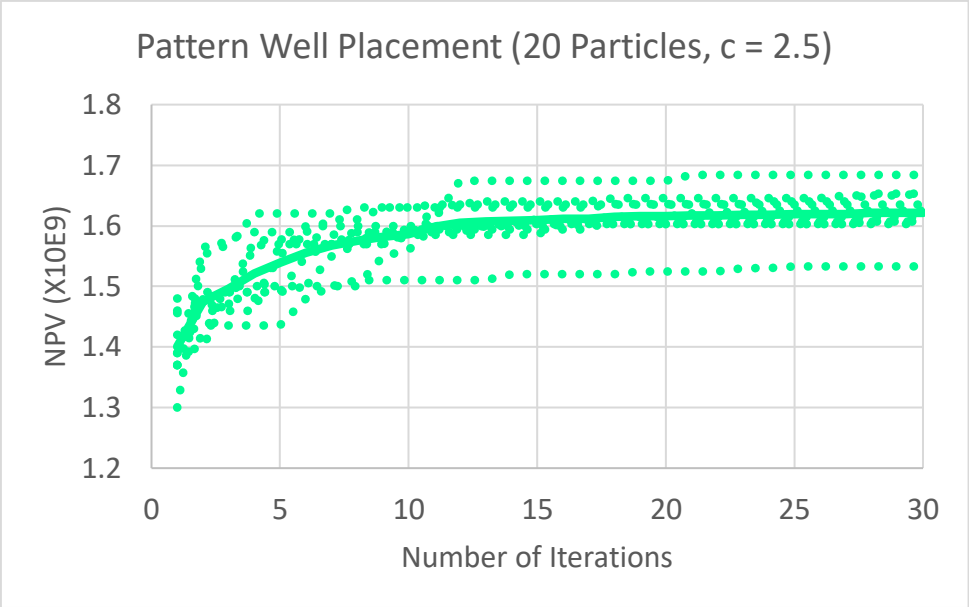

Figure 55 BHPSO Pattern Water Injection Results with c = 2.5 – LDIW

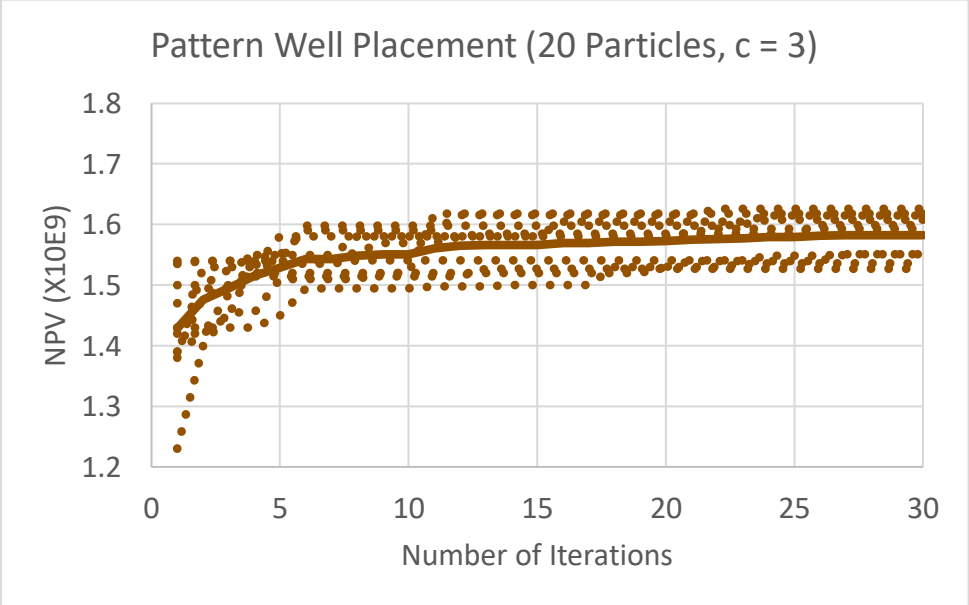

Figure 56 BHPSO Pattern Water Injection Results with c = 3 – LDIW

Furthermore, the main characteristic of the linearly decreasing inertia weight strategy, as stated in section 1.3.1.1., can be seen in Figure 57, Figure 58, and Figure 59, which is that, at the beginning, the algorithm exhibits an exploration ability in order to find a good seed, and then towards the end the algorithm exhibits a more exploitation

ability to fine tune the local area around the seed. Moreover, Figure 57 through Figure 59 display particle behavior for $c_p = c_g = 0.5$, 0.775 and 1 respectively, while Figure 60, Figure 61, and Figure 62 display the particle behavior for $c_p = c_g = 2$, 2.5 and 3 respectively, which do not yet display the characteristic mentioned above. Note that each of the figures below is representative of all 10 runs that were carried out for each acceleration coefficient value.

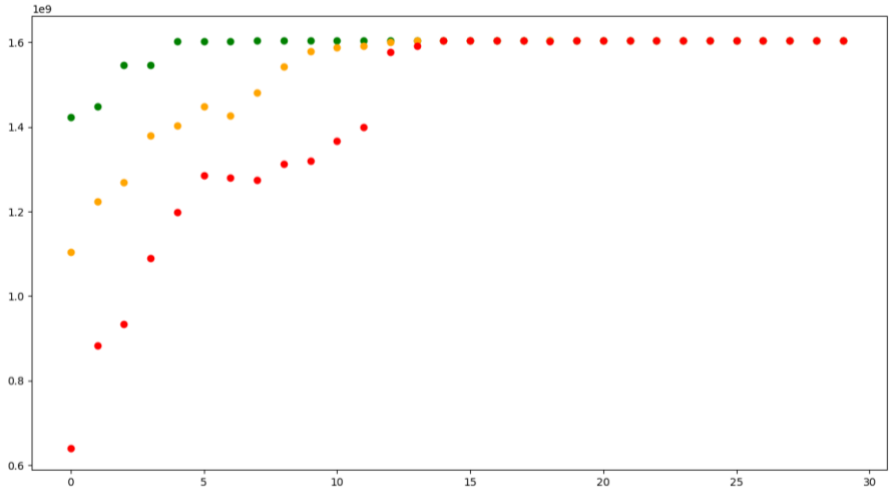

Figure 57 Representative BHPSO Performance of a LDIW with c = 0.5

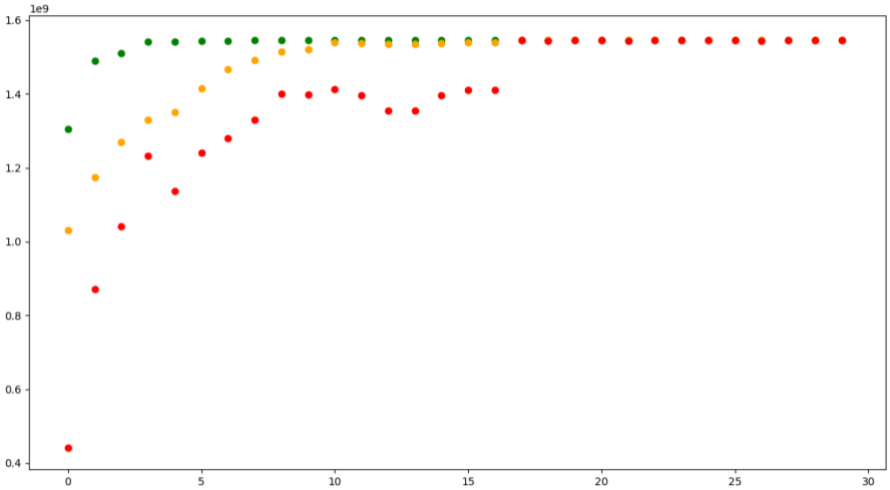

Figure 58 Representative BHPSO Performance of a LDIW with c = 0.775

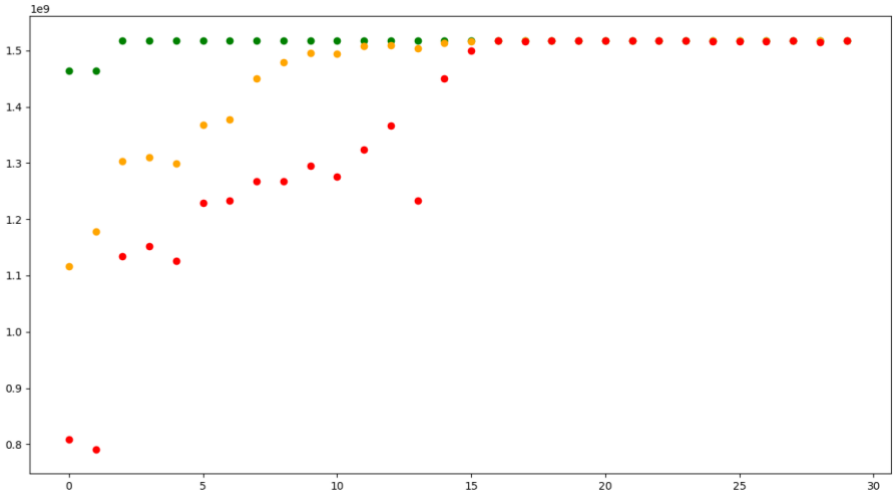

Figure 59 Representative BHPSO Performance of a LDIW with c = 1

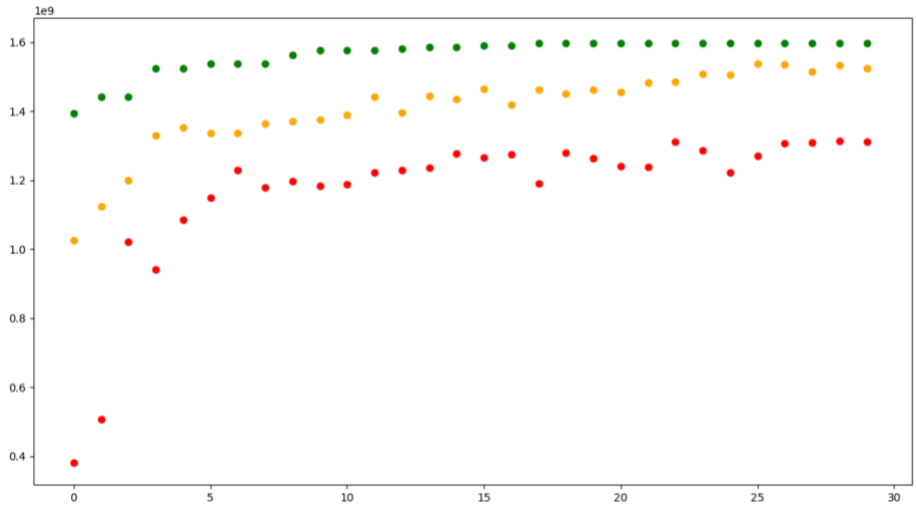

Figure 60 Representative BHPSO Performance of a LDIW with c = 2

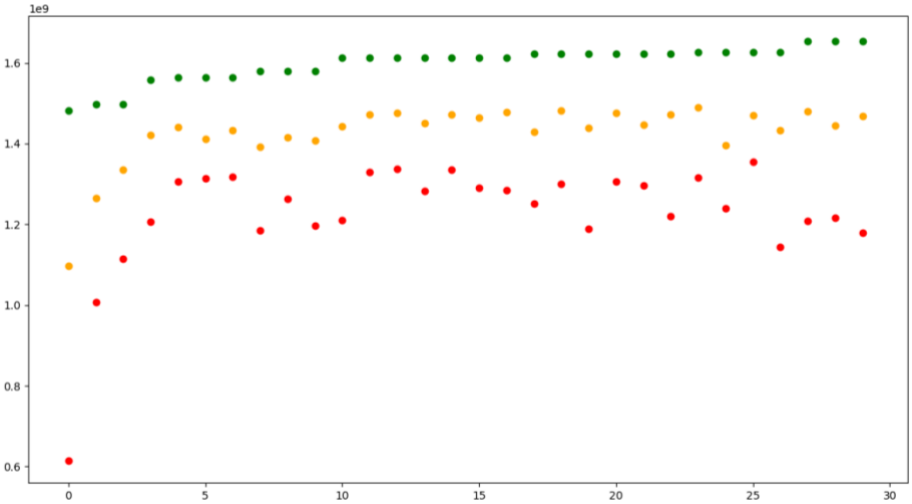

Figure 61 Representative BHPSO Performance of a LDIW with c = 2.5

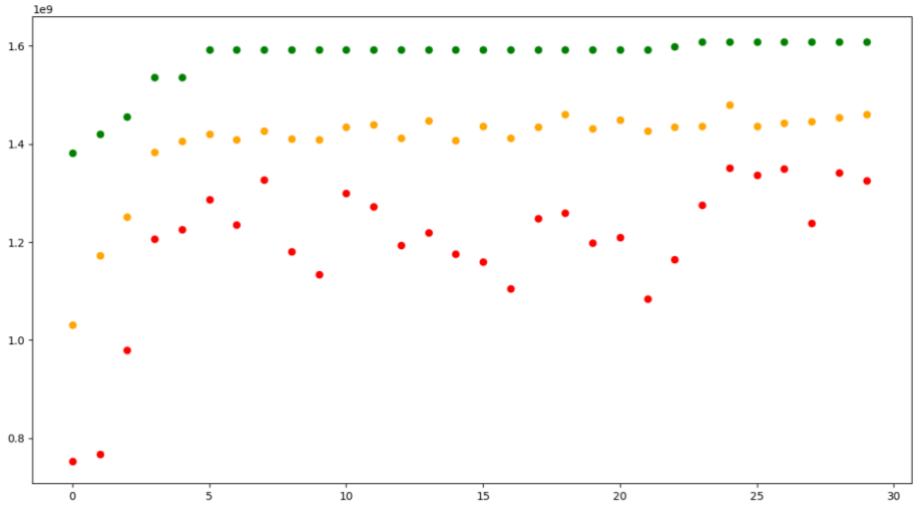

Figure 62 Representative BHPSO Performance of a LDIW with c = 3

4.3.2. LDIW Testing

In order to further assess the characteristics of a LDIW strategy, a study on the PUNQ-S3 field was carried out, for both pattern and peripheral water injection schemes, in which the iterations were increased from 30 to 100 and repeated 10 times. The obtained results (LDIW results) are compared with those in section 4.2. (CIW results) in terms of average NPV, redundancy, and convergence.

It can be seen in Figure 44 and Figure 63 (Pattern water injection scheme), and Figure 46 and Figure 64 (Peripheral water injection scheme) that in terms of average NPV and redundancy, for both injection schemes, that both inertia weight strategies returned comparable results. Where the case of a pattern water injection scheme with a CIW returned an average NPV of $1616 MM, a pattern water injection scheme with a LDIW returned an average NPV of $1620 MM. Similarily, for a peripheral water injection scheme, a CIW strategy returned an average NPV of $1648 MM, while a LDIW strategy returned an average NPV of $1652 MM.

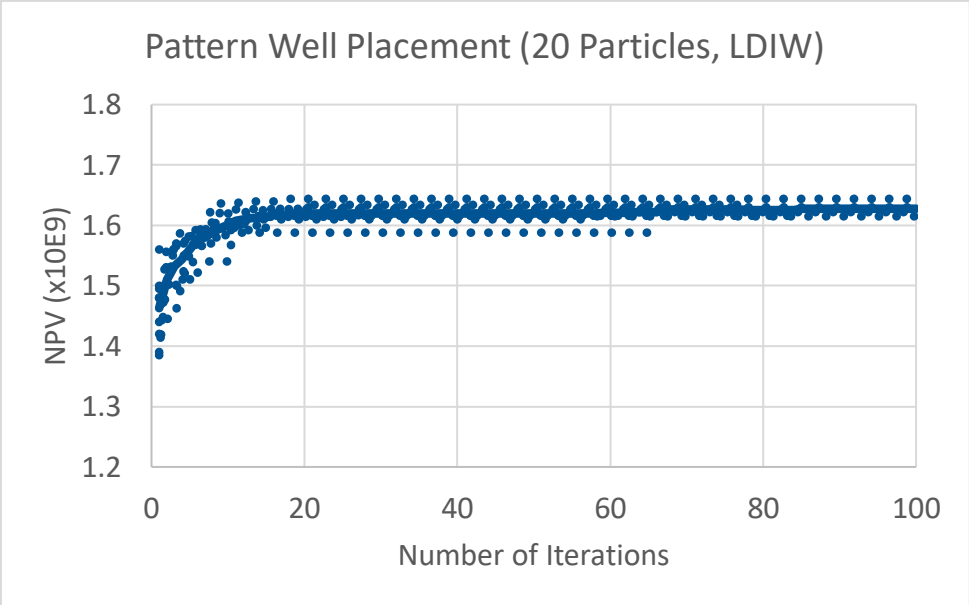

Figure 63 Pattern Water Injection Results for LDIW

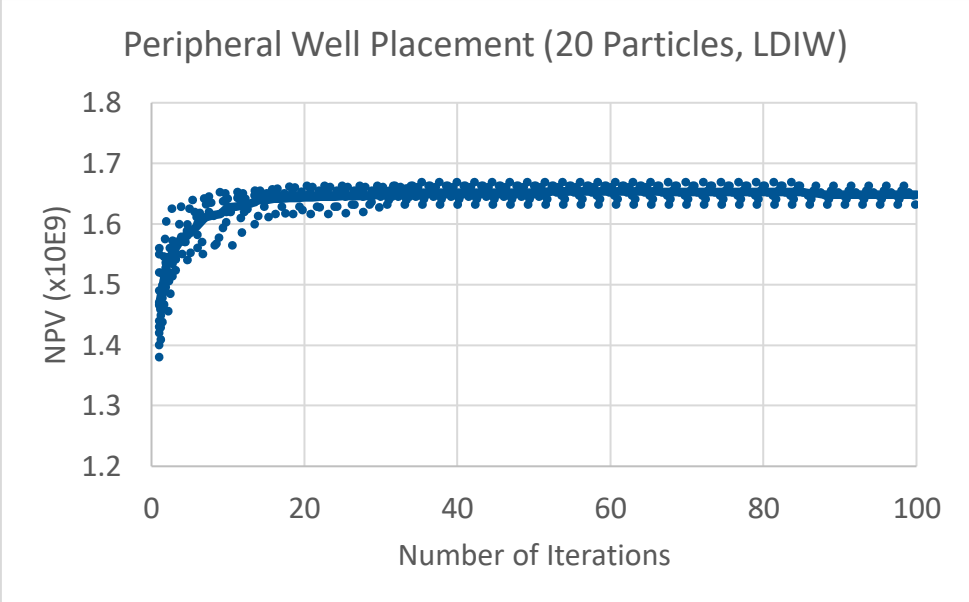

Figure 64 Peripheral Water Injection Results for LDIW

Moreover, the LDIW exploration-exploitation trade-off characteristic that was not observed in 30 iterations for accerlation coeffcients set to 2 (Figure 60) could be observed in the figures below. The main and most significant difference between a CIW and LWID strategy is that for the same average NPV, faster convergence is obtained,

hence decreasing simulation time. The aforementioned advantage can be seen in Figure 65, Figure 66, Figure 67, and Figure 68 where a representatitve BHPSO performance for each inertia weight strategy is displayed. Figure 65 displays a representative BHPSO performance of a pattern water injection scheme using a CIW strategy while Figure 66 displays a representative BHPSO performance of a pattern water injection scheme using a LDIW strategy. Likewise, Figure 67 displays a representative BHPSO performance of a peripheral water injection scheme using a CIW strategy while Figure 68 displays a representative optimization run of a peripheral water injection scheme using a LDIW strategy. It can be seen that a LDIW strategy reached very similar global best values as that of the CIW strategy, however the LDIW strategy allowed for shorter simulation time than those of the CIW strategy since the particles neared convergence at much earlier stages/iterations. In other words, a LDIW strategy returned identical results to those of a CIW strategy in a shorter amount of time.

Figure 65 Representative BHPSO Performance of a Pattern Injection Scheme – CIW

Figure 66 Representative BHPSO Performance of a Pattern Injection Scheme – LDIW

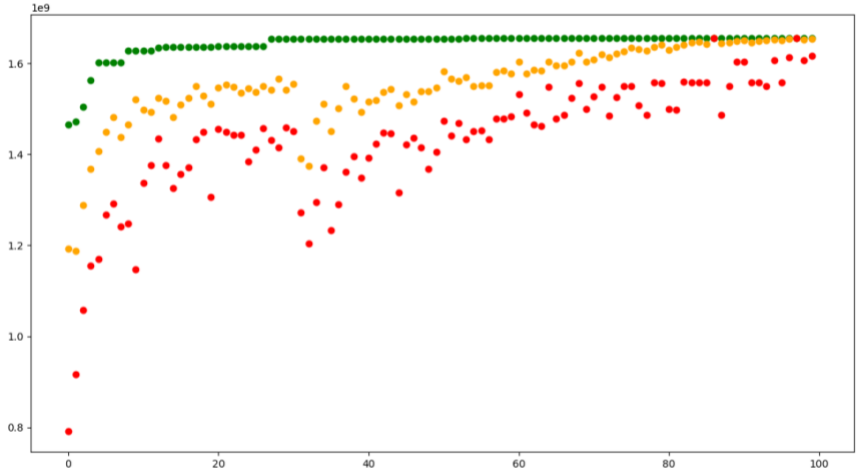

Figure 67 Representative BHPSO Performance of a Peripheral Injection Scheme – CIW

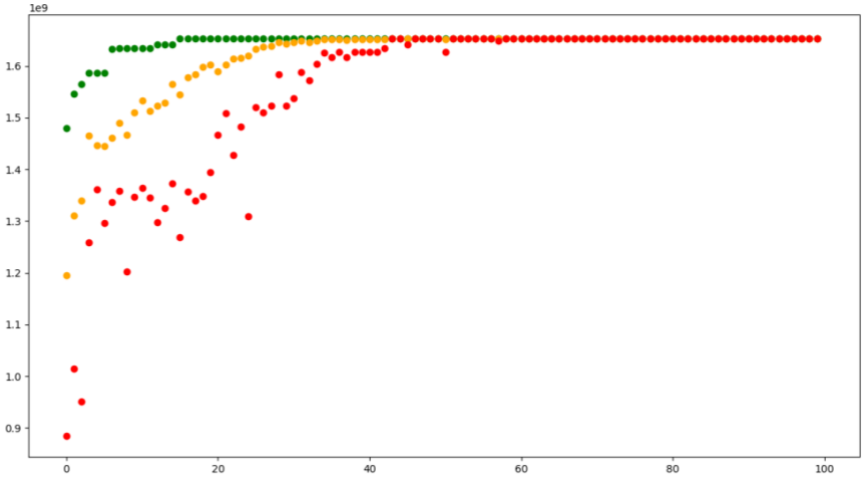

Figure 68 Representative BHPSO Performance of a Peripheral Injection Scheme – LDIW

CHAPTER 5

CONCLUSION

In this study, a peripheral water injection scheme was introduced to the black hole particle swarm optimizer since, depending on the field of study, it might be a more suitable development scenario than pattern water injection. The developed optimization method was implemented, tested and verified on both the Olympus and PUNQ-S3 fields. It should be noted that implementing the BH (manual input) on the Olympus and PUNQ-S3 fields resulted in NPVs of $817 MM (Figure 30) and $1352 MM (Figure 33), respectively, for a peripheral injection scheme, while, on the other hand, implementing the BHPSO (optimizing input), using only 5 particles, resulted in a 17-25% (Figure 20, Figure 21, and Figure 22) increase in the NPV for the Olympus field, and a 7-15% (Figure 23, Figure 24, and Figure 25) increase in the NPV for the PUNQ-S3 field.

The new black holing technique (region search) was tested on the PUNQ-S3 reservoir model, and its results were verified using the Olympus reservoir model. For a peripheral water injection scheme, results showed that the placement of injectors on the KH map using a region search method outperformed those of placing the injectors on the KH map using a point search method. As for the placement of producers on the NHCT map, the NPV results returned were in close proximity, however, a region search method depicted increased system complexity and simulation time. Similarly, for a pattern water injection scheme, the point search technique outmatched the region search technique in terms of system complexity and simulation time.

The convergence criteria of PSO was also addressed in this study which first included a sensitivity analysis on the swarm size (5,10,15 and 20 particles), however, a maximum of 20 particles was used due to system limitations (number of available

licenses). For both pattern and peripheral injection schemes, results displayed, in terms of NPV redundancy, that a swarm size of 20 particles would be the best swarm size to use to carry out testing. It should be noted that redundant NPV results are an indication of reliability, while the use of too few particles would result in the algorithm getting trapped in a local optimum, hence decreasing reliability and leading to varying NPV results. The use of a swarm size of 5, 10, and 15 particles was disregarded due to the variation in the NPV results which lead to decreased reliability. Moreover, while the use of a higher number of particles could result in better results since the particles would be sampling the search space more thoroughly, the function evaluation requirements would increase and slow down the algorithm. A balance between the number of particles and simulation time needs to be found.

The Inertia weight, another algorithmic parameter of PSO, was changed from a Constant Inertia Weight (CIW) to a Linearly Decreasing Inertia Weight (LDIW). The CIW used in the original BHPSO has a constant inertia weight value of 0.721 and acceleration factor values equivalent to 1.1931. As for a LDIW strategy, the inertia weight value varied from 0.9 to 0.4 across the iterations, while a sensitivity analysis was conducted on the acceleration factors ($c_p = c_g$) for values of 0.5, 0.775, 1, 2, 2.5 and 3. The optimal acceleration factor value with regard to NPV reliability was: $c_p = c_g = 2$. The LDIW showed improved results in terms of convergence over the CIW which included: faster convergence and fine-tuning of the local search.

Future work includes: (1) sensitivity analysis on the number of particles with regards to other fields so that the swarm size to be used in accordance with BHPSO can be verified (20 particles), (2) testing the LDIW on the Olympus field, (3) and then comparing the LDIW strategy to other inertia weight strategies, listed in chapter 1, by

implementing them in the BHPSO algorithm and testing them on the PUNQ-S3 and Olympus fields.

REFERENCES

[1] Harb, A., Kassem, H., & Ghorayeb, K. (2019). Black hole particle swarm optimization for well placement optimization. *Computational Geosciences,* doi:10.1007/s10596-019-09887-8

[2] Rezaee, R. (2015). *Fundamentals of gas shale reservoirs*. Wiley. Retrieved from https://ebookcentral-proquest-com.ezproxy.aub.edu.lb

[3] Manrique, E., & Alvarado, V. (2010). *Enhanced oil recovery: field planning and development strategies– 1. Reservoir Development Plans.* Elsevier. Retrieved from https://app.knovel.com/hotlink.pdf/id:kt00A21N53/enhanced-oil-recovery/reservoir-development

[4] Rostamian, A., Jamshidi, S., & Zirbes, E. (2019). The development of a novel multi-objective optimization framework for non-vertical well placement based on a modified non-dominated sorting genetic algorithm-II. *Computational Geosciences,* doi: 10.1007/s10596-019-09863-2

[5] Islam, J., Vasant, P. M., Negash, B. M., Laruccia, M. B., Myint, M., & Watada, J. (2020). A holistic review on artificial intelligence techniques for well placement optimization problem. *Advances in Engineering Software*, *141*, 102767. doi: 10.1016/j.advengsoft.2019.102767

[6] Okoro, E. E., Agwu, O. E., Olatunji, D., & Orodu, O. D. (2019). Artificial Bee Colony ABC a Potential for Optimizing Well Placement – A Review. *SPE Nigeria Annual International Conference and Exhibition*. doi: 10.2118/198729-ms

[7] Onwunalu, J. E., & Durlofsky, L. J. (2009). Application of a particle swarm optimization algorithm for determining optimum well location and type. *Computational Geosciences*, *14*(1), 183–198. doi: 10.1007/s10596-009-9142-1

[8] Onwunalu, J. E., & Durlofsky, L. (2011). A New Well-Pattern-Optimization Procedure for Large-Scale Field Development. *SPE Journal*, *16*(03), 594–607. doi: 10.2118/124364-pa

[9] Zhang, L., Zhang, K., Chen, Y., Li, M., Yao, J., Li, L., & Lee, J. (2015). Smart Well Pattern Optimization Using Gradient Algorithm. *Journal of Energy Resources Technology*, *138*(1). doi: 10.1115/1.4031208

[10] Nozohour-Leilabady, B., & Fazelabdolabadi, B. (2016). On the application of artificial bee colony (ABC) algorithm for optimization of well placements in fractured reservoirs; efficiency comparison with the particle swarm optimization (PSO) methodology. *Petroleum*, *2*(1), 79–89. doi: 10.1016/j.petlm.2015.11.004

[11] Udoeyop, S. U., Oboh, I. O., & Afiakinye, M. O. (2018). Algorithms for the Optimization of Well Placements—A Comparative Study. *Advances in Chemical Engineering and Science*, *08*(02), 101–111. doi: 10.4236/aces.2018.82007

[12] Lyons, W. C., Plisga, G.J., Lorenz, M. D. (2016). *Standard Handbook of Petroleum and Natural Gas Engineering (3rd Edition)* – 5.8.4.2 *Injection Well Placement.* (pp. 177-207). Elsevier. Retrieved from https://app.knovel.com/hotlink.pdf/id:kt010UZCU4/standard-handbook-petroleum/injection-well-placemenent

[13] Fanchi, J. R., & Christiansen, R. L. (2017). *Introduction to petroleum engineering*. John Wiley & Sons. Retrieved

from https://app.knovel.com/hotlink/pdf/id:kt011HPN82/introduction-petroleum/life-cycle-reservoir

[14] Bret-Rouzaut, Nadine, Favennec, Jean-Pierre. (2011). *Oil and Gas Exploration and Production - Reserves, Costs, Contracts (3rd Edition Revised and Updated).* Editions Technip. Retrieved from https://app.knovel.com/hotlink/pdf/id:kt00B0LGIC/oil-gas-exploration-production/recovery-mechanisms

[15] Bibars, O., & Hanafy, H. (2004). Waterflood Strategy - Challenges and Innovations. *Abu Dhabi International Conference and Exhibition*. doi: 10.2118/88774-ms

[16] Ahmed, T. (2019). *Reservoir Engineering Handbook (5th Edition)* Elsevier. Retrieved from https://app.knovel.com/hotlink/pdf/id:kt0123KHT2/reservoir-engineering/water-flooding-patterns

[17] Satter, A., Iqbal, G. M., & Buchwalter, J. L. (2008). *Practical enhanced reservoir engineering: assisted with simulation software*. PennWell. Retrieved from https://app.knovel.com/hotlink/pdf/id:kt0087RTS4/practical-enhanced-reservoir/waterflood-challenges

[18] Kuku, A., Omotayo-Johnson, M., Achinivu, O., Awotiku, O., & Oyegwa, A. (2019). Waterflood Management in Spring Field. *SPE Nigeria Annual International Conference and Exhibition*. doi: 10.2118/198810-ms

[19] Chetri, H., Clark, R. A., Al-Dashti, H., Sturrock, D., Al-Roweyah, A., & Al-Mufarej, M. (2005). Water Flooding a Heterogeneous Clastic Upper Burgan Reservoir in North Kuwait: Tackling the Reservoir Management & Injectivity Challenges. *SPE Middle East Oil and Gas Show and Conference*. doi: 10.2118/93548-ms

[20] El-hoshoudy, A. N. (2019) Evaluation of Waterflooding; Experimental and Simulation Overview. *Petroleum and Petrochemical Engineering Journal.* doi: 10.23880/ppej-16000196

[21] Stephens, F. (1960). Peripheral and Line-Drive Water-Injection Projects. *Journal of Petroleum Technology*, *12*(12), 16–19. doi: 10.2118/1504-g

[22] Ghauri, U. M. K., Agrawal, P., Kumar, A., Uijttenhout, M., & Draoui, E. H. (2019). Evolution of the Field Development Plan of High Permeability Multilayered Reservoir and Optimization of Injection Strategy. *SPE Gas & Oil Technology Showcase and Conference*. doi: 10.2118/198587-ms

[23] Konwar, L., Alowainati, E., Alanaisis, I., Nemmawi, N., & Michael, D. (2019). Understanding Mauddud Waterflood Performance in a Heterogeneous Carbonate Reservoir with Surveillance Data and Ensemble of Analytical Tools. *SPE Middle East Oil and Gas Show and Conference*. doi: 10.2118/195130-ms

[24] Yadav, A., Malkov, A., Omara, E., El-Hawari, A., Davudov, D., Danisman, Y., & Venkatraman, A. (2019). A New Continuous Waterflood Operations Optimization for a Mature Oil Field by using Analytical Workflows that Improve Reservoir Characterization. *SPE Gas & Oil Technology Showcase and Conference*. doi: 10.2118/198586-ms

[25] Rezaee Jordehi, A., & Jasni, J. (2013). Parameter selection in particle swarm optimisation: A survey. *Journal of Experimental & Theoretical Artificial Intelligence, 25*(4), 527-542. doi:10.1080/0952813x.2013.782348

[26] Y. Shi and R. Eberhart, "A modified particle swarm optimizer," 1998 IEEE International Conference on Evolutionary Computation Proceedings. IEEE World

Congress on Computational Intelligence (Cat. No.98TH8360), Anchorage, AK, USA, 1998, pp. 69-73, doi: 10.1109/ICEC.1998.699146

[27] Wang, D., Tan, D., & Liu, L. (2017;2018;). Particle swarm optimization algorithm: An overview. *Soft Computing (Berlin, Germany), 22*(2), 387-408. doi:10.1007/s00500-016-2474-6

[28] Ioan Cristian Trelea. (2003). The particle swarm optimization algorithm: convergence analysis and parameter selection. Information Processing Letters, 85(6), 317-325. doi: 10.1016/S0020-0190(02)00447-7

[29] Nickabadi, A., Ebadzadeh, M. M., & Safabakhsh, R. (2011). A novel particle swarm optimization algorithm with adaptive inertia weight. *Applied Soft Computing, 11*(4), 3658-3670. doi:10.1016/j.asoc.2011.01.037

[30] Meziane, M. A., Mouloudi, Y., Bouchiba, B., & Laoufi, A. (2019). Impact of inertia weight strategies in particle swarm optimization for solving economic dispatch problem. *Indonesian Journal of Electrical Engineering and Computer Science, 13*(1), 377. doi:10.11591/ijeecs.v13.i1.pp377-383

[31] Bansal, J. C., Singh, P. K., Saraswat, M., Verma, A., Jadon, S. S., & Abraham, A. (2011). Inertia Weight strategies in Particle Swarm Optimization. *2011 Third World Congress on Nature and Biologically Inspired Computing*. doi:10.1109/nabic.2011.6089659

[32] Gupta, Indresh Kumar, et al. "Particle Swarm Optimization with Selective Multiple Inertia Weights." *2017 8th International Conference on Computing, Communication and Networking Technologies (ICCCNT)*, 2017, doi:10.1109/icccnt.2017.8204132.

[33] Kennedy J, Eberhart R. Particle swarm optimization, IEEE international of first conference on neural networks. Perth, Australia: IEEE Press; 1995.

[34] Shi Y., Eberhart R.C. (1998) Parameter selection in particle swarm optimization. In: Porto V.W., Saravanan N., Waagen D., Eiben A.E. (eds) Evolutionary Programming VII. EP 1998. Lecture Notes in Computer Science, vol 1447. Springer, Berlin, Heidelberg. https://doi.org/10.1007/BFb0040810

[35] Y. Shi and R. C. Eberhart, "Empirical study of particle swarm optimization," Proceedings of the 1999 Congress on Evolutionary Computation-CEC99 (Cat. No. 99TH8406), Washington, DC, USA, 1999, pp. 1945-1950 Vol. 3, doi: 10.1109/CEC.1999.785511.

[36] Arumugam, M. S., & Rao, M. V. C. (2006). On the performance of the particle swarm optimization algorithm with various inertia weight variants for computing optimal control of a class of hybrid systems. *Discrete Dynamics in Nature and Society*, *2006*, 1–17. https://doi.org/10.1155/ddns/2006/79295

[37] Umapathy, Prabha, et al. “Particle Swarm Optimization with Various Inertia Weight Variants for Optimal Power Flow Solution.” *Discrete Dynamics in Nature and Society*, vol. 2010, 2010, pp. 1–15., doi:10.1155/2010/462145.

[38] Y. Feng, G. Teng, A. Wang and Y. Yao, "Chaotic Inertia Weight in Particle Swarm Optimization," Second International Conference on Innovative Computing, Informatio and Control (ICICIC 2007), Kumamoto, 2007, pp. 475-475, doi: 10.1109/ICICIC.2007.209.

[39] Yang, C., Hsiao, C., & Chuang, L. Linearly Decreasing Weight Particle Swarm Optimization with Accelerated Strategy for Data Clustering.

[40] Carlisle, A. and Dozier, G. (2001), An off-the-shelf pso, In: Proceedings of the Workshop on Particle Swarm Optimization, Purdue School of Engineering and Technology, Indianapolis, USA.

[41] Schutte JF, Groenwold AA (2005) A study of global optimization using particle swarms. J Glob Optim 31:93–108

[42] Clerc, M. 2006b. Stagnation Analysis in Particle Swarm Optimisation or What Happens When Nothing Happens. Technical Report CSM-460, Department of Computer Science, University of Essex, Essex, UK (August 2006).

[43] Ding, S., Lu, R., Xi, Y., Liu, G., & Ma, J. (2020). Efficient well placement optimization coupling hybrid objective function with particle swarm optimization algorithm. *Applied Soft Computing*, *95*, 106511. https://doi.org/10.1016/j.asoc.2020.106511

[44] Ding, Shuai-wei & Yuan, Yi-dong & Xi, Yi & Fan, Qian-qian & Liu, Guang-wei & Wang, Shuo-liang & Ma, Jin-feng. (2020). Optimization of Well Placement by PSO Assisted by Quality Map and Gompertz-Based Grey Model. 10.1007/978-981-15-2485-1_142.

[45] Onwunalu, J. E., & Durlofsky, L. J. (2009). Application of a particle swarm optimization algorithm for determining optimum well location and type. *Computational Geosciences*, *14*(1), 183–198. https://doi.org/10.1007/s10596-009-9142-1

[46] Naderi, M., & Khamehchi, E. (2017). Well placement optimization using metaheuristic bat algorithm. *Journal of Petroleum Science and Engineering*, *150*, 348-354. doi:10.1016/j.petrol.2016.12.028

[47] Jesmani, M., Bellout, M. C., Hanea, R., & Foss, B. (2016). Well placement optimization subject to realistic field development constraints. *Computational Geosciences*, *20*(6), 1185–1209. https://doi.org/10.1007/s10596-016-9584-1

[48] Nwankwor, E., Nagar, A. K., & Reid, D. C. (2012). Hybrid differential evolution and particle swarm optimization for optimal well placement. *Computational Geosciences*, *17*(2), 249–268. https://doi.org/10.1007/s10596-012-9328-9

[49] Schulze-Riegert, R., Nwakile, M., Skripkin, S. *et al.* (2019) Olympus challenge—standardized workflow design for field development plan optimization under uncertainty. *Comput Geosci*. doi:10.1007/s10596-019-09905-9

[50] Chang, Y., Lorentzen, R. J., Nævdal, G., & Feng, T. (2019). OLYMPUS optimization under geological uncertainty. *Computational Geosciences*, , 1-16. doi:http://dx.doi.org.ezproxy.aub.edu.lb/10.1007/s10596-019-09892-x

[51] Barker, W.J., Cuypers, M., Holden, L., 2001. Quantifying uncertainty in production forecasts: another look at the PUNQ-S3 problem,. SPE J., 433.

[52] Floris, F.J.T., Bush, M.D., Cuypers, M., Roggero, F., Syversveen, A.-R., 2001. Methods for quantifying the uncertainty of production forecasts: a comparative study,. Pet. Geosci. 7, S87